NPS ARCHIVE
1999.09
CARINO, D.

DUDLEY KNOX LIBRARY
NAVAL POSTGRADUATE SCHOOL
MONTEREY CA 93943-5101

NAVAL POSTGRADUATE SCHOOL
Monterey, California

THESIS

ANALYSIS OF ENVIRONMENTAL INFLUENCES ON BROADBAND EXPLOSIVE TRANSMISSION LOSS SPECTRA NEAR THE MID-ATLANTIC BIGHT

by

Dominic Carino

September 1999

Thesis Advisor: Kevin B. Smith
Second Reader: Mitch Shipley

Approved for public release; distribution is unlimited.

REPORT DOCUMENTATION PAGE

Form Approved
OMB No. 0704-0188

Public reporting burden for this collection of information is estimated to average 1 hour per response, including the time for reviewing instruction, searching existing data sources, gathering and maintaining the data needed, and completing and reviewing the collection of information. Send comments regarding this burden estimate or any other aspect of this collection of information, including suggestions for reducing this burden, to Washington headquarters Services, Directorate for Information Operations and Reports, 1215 Jefferson Davis Highway, Suite 1204, Arlington, VA 22202-4302, and to the Office of Management and Budget, Paperwork Reduction Project (0704-0188) Washington DC 20503.

1. AGENCY USE ONLY *(Leave blank)*	2. REPORT DATE	3. REPORT TYPE AND DATES COVERED
	September 1999	Master's Thesis

4. TITLE AND SUBTITLE	5. FUNDING NUMBERS
Analysis of Environmental Influences on Broadband Explosive Transmission Loss Spectra Near the Mid-Atlantic Bight	
6. AUTHOR(S) Dominic Carino	
7. PERFORMING ORGANIZATION NAME(S) AND ADDRESS(ES) Naval Postgraduate School Monterey, CA 93943-5000	8. PERFORMING ORGANIZATION REPORT NUMBER
9. SPONSORING / MONITORING AGENCY NAME(S) AND ADDRESS(ES)	10. S PONSORING / MONITORING AGENCY REPORT NUMBER

11. SUPPLEMENTARY NOTES

The views expressed in this thesis are those of the author and do not reflect the official policy or position of the Department of Defense or the U.S. Government.

12a. DISTRIBUTION / AVAILABILITY STATEMENT	12b. DISTRIBUTION CODE
Approved for public release; distribution unlimited.	

13. ABSTRACT *(maximum 200 words)*

Under the sponsorship of the Office of Naval Research (ONR), an integrated acoustic and oceanographic field experiment was conducted jointly by the Naval Postgraduate School (NPS), the Woods Hole Oceanographic Institution (WHOI), and the University of Rhode Island in the Middle Atlantic Bight (MAB) to study the propagation of sound from the continental slope onto the continental shelf. The primary goal of this thesis is to examine the influence of environmental factors on broadband transmission loss (TL) spectra near the shelf break by analyzing the power spectral density of Signal Underwater Sound (SUS) transmissions. Measured broadband spectra are compared to numerical solutions in an attempt to determine which environmental factors dominate the TL structure.

14. SUBJECT TERMS broadband transmission loss (TL), signal underwater sound (SUS), measured broadband spectra	15. NUMBER OF PAGES 66
	16. PRICE CODE

17. SECURITY CLASSIFICATION OF REPORT	18. SECURITY CLASSIFICATION OF THIS PAGE	19. SECURITY CLASSIFICATION OF ABSTRACT	20. LIMITATION OF ABSTRACT
Unclassified	Unclassified	Unclassified	UL

NSN 7540-01-280-5500

Standard Form 298 (Rev. 2-89)
Prescribed by ANSI Std. 239-18

Approved for public release; distribution is unlimited.

ANALYSIS OF ENVIRONMENTAL INFLUENCES ON BROADBAND EXPLOSIVE TRANSMISSION LOSS SPECTRA NEAR THE MID ATLANTIC BIGHT

Dominic Carino
Major, Canadian Air Force
Adv. B.A., University of Manitoba, 1990

Submitted in partial fulfillment of the
requirements for the degree of

MASTER OF SCIENCE IN ENGINEERING ACOUSTICS

from the

NAVAL POSTGRADUATE SCHOOL
September 1999

DUDLEY KNOX LIBRARY
NAVAL POSTGRADUATE SCHOOL
MONTEREY CA 93943-5101

ABSTRACT

Under the sponsorship of the Office of Naval Research (ONR), an integrated acoustic and oceanographic field experiment was conducted jointly by the Naval Postgraduate School (NPS), the Woods Hole Oceanographic Institution (WHOI), and the University of Rhode Island in the Middle Atlantic Bight (MAB) to study the propagation of sound from the continental slope onto the continental shelf. The primary goal of this thesis is to examine the influence of environmental factors on broadband transmission loss (TL) spectra near the shelf break by analyzing the power spectral density of Signal Underwater Sound (SUS) transmissions. Measured broadband spectra are compared to numerical solutions in an attempt to determine which environmental factors dominate the TL structure.

TABLE OF CONTENTS

LIST OF FIGURES

LIST OF TABLES

ACKNOWLEDGMENTS

I would like to take this opportunity to express my sincere gratitude and appreciation to those who helped me throughout this thesis project and during my time at NPS. First, I would like to thank Professor Kevin Smith for providing the continuous guidance, direction, technical support, and vast knowledge to help me through the thesis process. Without his abundance of patience and assistance, this thesis project could not have been completed. Secondly, I thank CDR Mitch Shipley, who was always available for much needed advice and assistance through the thesis writing process. To Professor Sanders, the academic advisor, who provided wisdom and counseling during each quarter so that my learning experience was maximized, I thank you.

I also thank my fellow lab partners for providing technical assistance with the technical aspects of software manipulation when needed. This saved me many hours of trial and error procedures to achieve the required results. Many thanks to my classmates, who helped with the most challenging academic venture in my career at NPS.

A special thank you goes to Nancy Sharrock for spending many hours in typing the initial thesis preparation. Also, a special thank you to the International Office faculty, especially Colonel Roser for his candid remarks when needed, and to Cindy Graham, who through her untiring efforts made my family's stay at NPS very rewarding.

Finally, and most importantly, I wish to thank my son Andrew, my daughters Selina, Leandra, and Claudia, and my wife Donna for always being there. I could not have completed my studies without your continuous support, untiring patience, and love. Thank you with all my heart!

I. INTRODUCTION

A. BACKGROUND

The end of the Cold War has brought a shift in Naval USW operations from deep water into littoral regions and thus the need to study the behaviour of sound propagation in this new environment. With the rapidly increasing involvement of the US Navy in and around third world countries' littoral regions, there is a requirement to understand the effects of the ocean environment on undersea sound and undersea warfare (USW) operations. These ever changing challenges require extensive acoustic environmental knowledge in all probable shallow water operating areas so that the Navy can operate effectively. While it is not feasible to study all significant regions due to political, fiscal, and human resource constraints, one study called the Mid-Atlantic Bight (MAB) Shelf Break Primer experiment (or simply Primer) was conducted in 1996 in the littoral area located southeast of Long Island, New York (Fig. 1.1).

B. OBJECTIVES OF THE MID-ATLANTIC BIGHT EXPERIMENT

One of the main goals of the Primer experiment was to quantify shelf break frontal variability and its connection with adjacent slope water circulation and to determine this variability on sound propagation from the continental slope onto the shelf (Smith, et al., 1996). The study also attempted to provide a detailed time series of oceanographic conditions along typical acoustic paths by using moored acoustical arrays. Temperature structure of the ocean environment was determined using acoustic tomography techniques (Pickart, et

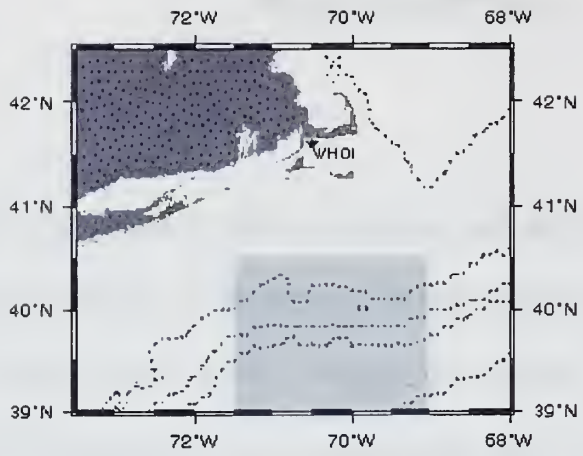

PRIMER III Field Study July--August, 1996

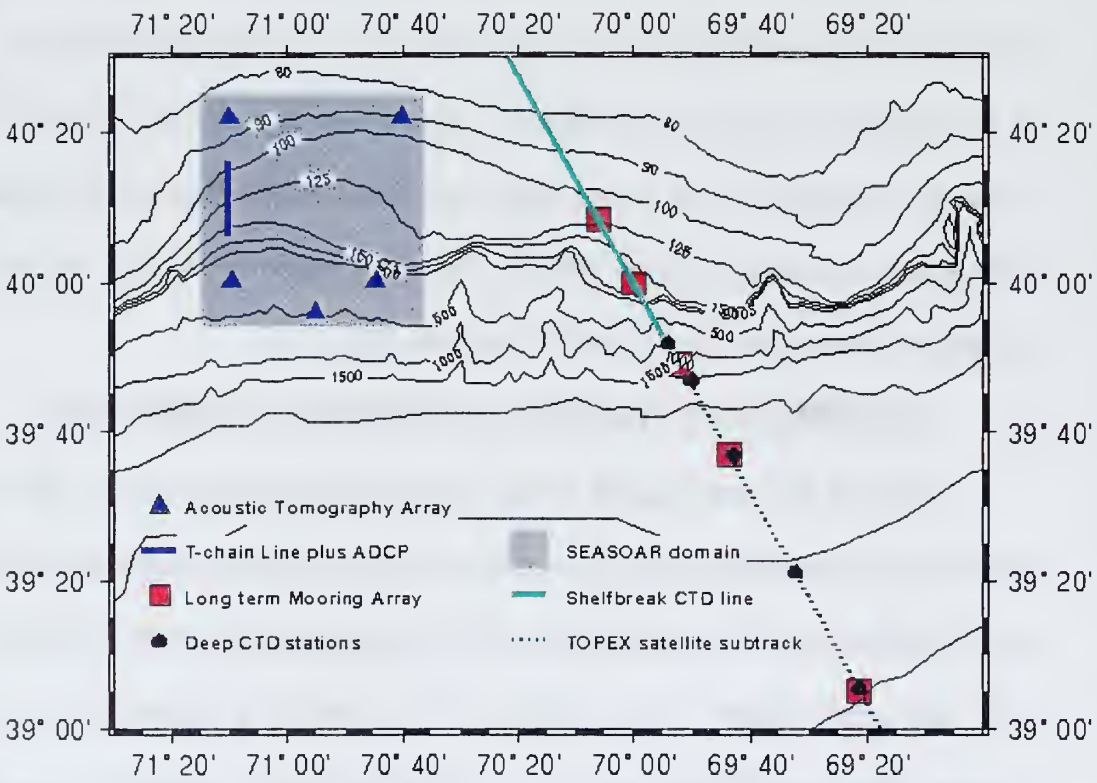

Figure 1.1. Arrangement of acoustical elements of the MAB experiment (from WHOI, 1996).

al., 1996). The Primer experiment has also been the impetus for study in the area of geoacoustic inversions – extraction of bottom sound speed and density from in-situ acoustic data (Rojas, 1998, Smith et al., 1999, and Potty et al., 1999). In addition, as part of the study requirements, Signal Underwater Sound (SUS) charges were used to provide a diversity of frequencies and broadband source locations. Small explosive charges have been used extensively in underwater acoustics for measuring quantities such as propagation loss, reverberation, and bottom reflection loss (Hannay et al., 1998). This SUS data will provide the measured signals for this thesis.

C. THESIS OBJECTIVES

The primary goal of this study is to determine the dominant factors which influence broadband acoustic propagation near the MAB Shelf Break region. In order to achieve this, several types of analysis must be performed. To estimate average transmission loss (TL) values as a function of frequency from the various SUS locations to the northwest vertical line array (NW VLA), the energy flux spectra of the received signal must be computed. In addition, the source spectra of the 1.8 lb. explosive SUS must be defined. Finally, these in-situ TL results will be compared to parabolic equation (PE) propagation model results to ascertain what features of the acoustic environment are primarily responsible for the observed trends in the data.

D. THESIS OUTLINE

The remainder of the thesis consists of five chapters. Chapter II describes the Primer experiment in more detail including the environment, data recording

devices and methods, and data processing criteria for signal processing. Chapter III describes the Monterey-Miami Parabolic Equation (MMPE) numerical model used in the thesis to predict TL values used to compare with the in-situ TL results. This model is an upgraded version of the University of Miami Parabolic Equation (UMPE) model developed by Smith and Tappert (1993). Chapter IV describes the environmental models and processing techniques used to find ambient noise spectra, sound speed profiles, SUS spectra and estimates of average TL, and average TL predictions based on model results. Chapter V presents the analysis and compares measured TL results to that of model TL results to determine what environmental factors, if any, most significantly affect the findings. Chapter VI provides a summary of the results and conclusions.

II. ENVIRONMENTAL/EXPERIMENTAL DESCRIPTION

A. PHYSICAL ENVIRONMENT

The dominant feature of the Mid-Atlantic region off the eastern coast of the United States is the Mid-Atlantic Bight (MAB). The MAB underlies the coastal plain, continental shelf and upper part of the continental slope of the Middle Atlantic United States. This region extends more than 500 kilometers parallel with the shoreline between Cape Cod and Cape Hatteras. The seaward border of the MAB is a ridge of Mesozoic sedimentary rock that underlies the present upper continental slope. The Bight is at its widest off the coast of New Jersey and New York where it extends approximately 200 kilometers from the shoreline (Poag, 1979).

The geographical location of the MAB lends itself to a complex oceanographic structure with a maximum depth of approximately 200 meters on its seaward side and a depth of less than 50 meters over most of the Bight. This region is considered a shallow coastal water area. This physical feature, along with its proximity to the Gulf Stream, generates many characteristics unique to the MAB. Through the study of these complex regions, conclusions may be drawn that can be applied to other environmentally similar regions around the globe that may be of interest to the Navy for future operations.

B. EXPERIMENTAL DESCRIPTION

The Primer experiment was conducted in the northern portion of the region (see Fig. 1.1) and was a collaborative study between the Woods Hole

Oceanographic Institution (WHOI), the University of Rhode Island, and the Naval Postgraduate School (NPS). The experiment consisted of a summer and subsequent winter portion to fully gain a more comprehensive database of oceanographic environmental conditions. This thesis will focus on the summer cruise data only.

The summer portion of the Primer experiment was carried out from 19 July to 9 August 1996 aboard the R/V Endeavor. This was an intensive field study of the shelf break current south of Cape Cod during the strongly stratified summer season. The cruise included three major components: acoustic tomography, SeaSoar operations, and hydrography/tracers. SeaSoar is a mechanical fish-like sensor that generally undulated between the surface and a depth of 120 m, or 10 m above the bottom, towed behind the R/V Endeavor. It provided information on the water column properties during the experiment, including temperature and salinity as a function of depth.

The acoustic portion of the experiment consisted of four components: 1) the moored acoustic tomography sources, 2) the moored physical oceanography array, which provided detailed time series of the oceanographic conditions along the major acoustic path, 3) the broadband SUS shot source component, which provided a diversity of frequencies and source locations for various propagation studies, and 4) the moored vertical line arrays (VLA's) (Pickart, et al., 1996). On 27 July, a P-3 aircraft SUS drop flyover was conducted where multiple lines of SUS drops were deployed in the area and monitored by the VLA's moored on the shelf in approximately 85 m of water.

During a seven day period, SeaSoar operations were directed toward resolving thermohaline and velocity fields within the area where samples taken of the shelf break front allowed 0.5 km horizontal resolution for the first time (Pickart, et al., 1996). This resolution aided in the revelation of a complex frontal boundary, showing a sharp front that was affected by a warm eddy, and large horizontal temperature contrasts over relatively short distances. The deployment typically occupied four cross-shelf transects daily, roughly 45 km in length, which extended from the 85 m isobath to the 500 m isobath. SeaSoar data was used to determine typical sound speed profiles for the area, which in turn were used as input for the MMPE model. To achieve the objectives of this thesis, 22 broadband SUS shot transmissions from drop Run 1 and 11 SUS shots from drop Run 4 recorded at the NW VLA were selected from data provided by the Woods Hole Oceanographic Institution. The SUS charges were 1.8 lbs. of TNT explosive designed to detonate at a depth of 18.3 m. The sampling frequency of the SUS signal on the VLA was 3906.25 Hz. Using the same sampling frequency, the data was further processed at the University of Rhode Island into records of 8.3886 sec duration with a number of samples per record of 32768. This ensured that one record contained only one SUS explosion. The arrangement and location of the acoustical elements used for this study are shown in Fig. 2.1 including the NW VLA position, the N to S Run 1 SUS and W to E Run 4 SUS positions, and the positions of the SeaSor data used to calculate the required SSP's.

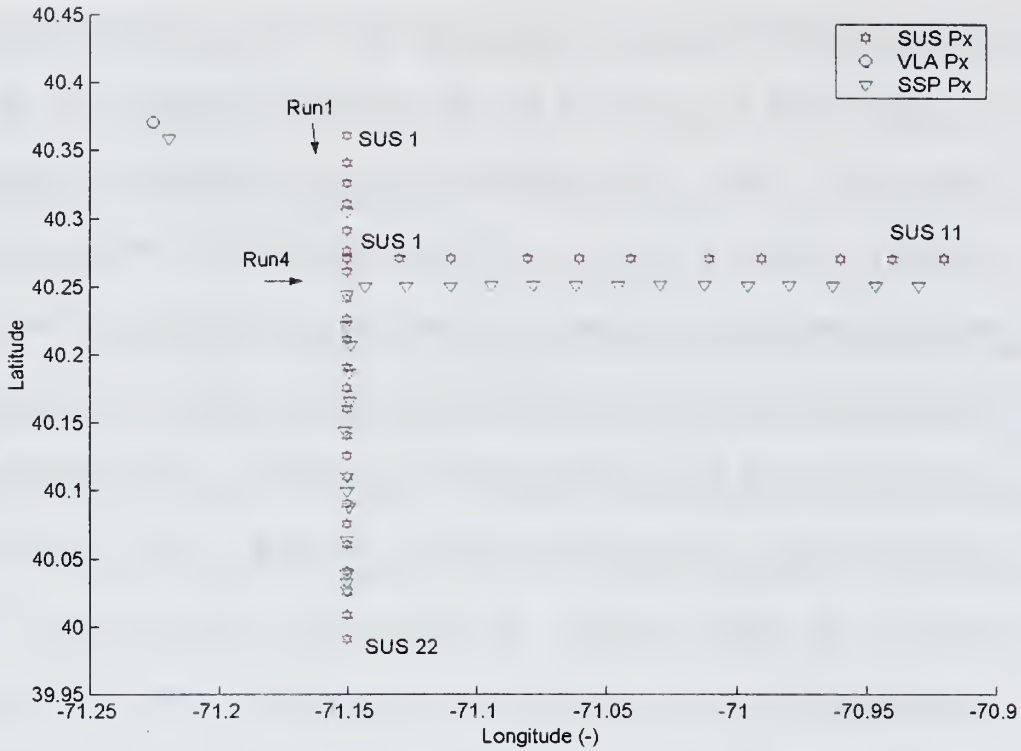

Figure 2.1. Acoustical elements used in the study.

Table 2.1 outlines the respective element positions and ranges to the receiving VLA for each aircraft SUS drop. Table 2.2 outlines the general positions of the SeaSoar data where SSP's were calculated and used as input for the model work.

The receiving VLA had hydrophones from 84 m depth up to 31.5 m with 3.5 m element separation for a total of 16 hydrophones. Unfortunately, on 27 July when the SUS were dropped, only the top 8 hydrophones were functional due to an electrical fuse malfunction. As a result, analysis of the SUS data was limited to the top 8 phones (Smith, et al., 1996). A more detailed discussion of the initial data manipulation for analysis and model input will be presented in Chapter IV.

Acoustical Element	Latitude	Longitude	Distance to VLA (km)
VLA	40°22.1′	-71°13.5′	
Run4 SUS1	40°16.1′	-71°09.1′	13.85
Run4 SUS2	40°16.1′	-71°07.7′	14.81
Run4 SUS3	40°16.1′	-71°06.3′	15.91
Run4 SUS4	40°16.1′	-71°04.9′	17.16
Run4 SUS5	40°16.1′	-71°03.5′	18.50
Run4 SUS6	40°16.1′	-71°02.1′	19.92
Run4 SUS7	40°16.1′	-71°00.7′	21.40
Run4 SUS8	40°16.1′	-70°59.2′	22.90
Run4 SUS9	40°16.1′	-70°57.8′	23.98
Run4 SUS10	40°16.1′	-70°56.4′	26.65
Run4 SUS11	40°16.1′	-70°55.0′	28.46
Run1 SUS1	40°21.6′	-71°09.1′	6.33
Run1 SUS2	40°20.5′	-71°09.1′	6.91
Run1 SUS3	40°19.5′	-71°09.1′	7.88
Run1 SUS4	40°18.5′	-71°09.1′	9.13
Run1 SUS5	40°17.5′	-71°09.1′	10.56
Run1 SUS6	40°16.5′	-71°09.1′	12.10
Run1 SUS7	40°15.5′	-71°09.1′	13.72
Run1 SUS8	40°14.5′	-71°09.1′	15.39
Run1 SUS9	40°13.5′	-71°09.1′	17.10
Run1 SUS10	40°12.5′	-71°09.1′	18.84
Run1 SUS11	40°11.5′	-71°09.1′	20.59
Run1 SUS12	40°10.5′	-71°09.1′	22.36
Run1 SUS13	40°09.5′	-71°09.1′	24.14
Run1 SUS14	40°08.5′	-71°09.1′	25.94
Run1 SUS15	40°07.5′	-71°09.1′	27.74
Run1 SUS16	40°06.5′	-71°09.1′	29.54
Run1 SUS17	40°05.5′	-71°09.1′	31.35
Run1 SUS18	40°04.5′	-71°09.1′	33.17
Run1 SUS19	40°03.5′	-71°09.1′	34.99
Run1 SUS20	40°02.5′	-71°09.1′	36.81
Run1 SUS21	40°01.5′	-71°09.1′	38.64
Run1 SUS22	40°00.5′	-71°09.1′	40.46

Table 2.1. Location of acoustical elements used in the experimental study.

SEASOR	Latitude	Longitude
Data for SSP Input		
Run 4 XY 482	40°14.9′	-71°09.0′
Run 4 XY 483	40°14.9′	-71°08.6′
Run 4 XY 484	40°14.9′	-71°07.6′
Run 4 XY 485	40°14.9′	-71°06.6′
Run 4 XY 486	40°14.9′	-71°05.6′
Run 4 XY 487	40°14.9′	-71°04.7′
Run 4 XY 488	40°14.9′	-71°03.7′
Run 4 XY 489	40°14.9′	-71°02.7′
Run 4 XY 490	40°14.9′	-71°01.7′
Run 4 XY 491	40°14.9′	-71°00.7′
Run 4 XY 492	40°14.9′	-70°59.7′
Run 4 XY 493	40°14.9′	-70°58.8′
Run 4 XY 494	40°14.9′	-70°57.8′
Run 4 XY 495	40°14.9′	-70°56.8′
Run 4 XY 496	40°14.9′	-70°55.8′
Run 1 XY 310	40°02.3′	-71°09.0′
Run 1 XY 316	40°06.6′	-71°09.0′
Run 1 XY 319	40°08.6′	-71°09.1′
Run 1 XY 321	40°09.9′	-71°09.0′
Run 1 XY 328	40°14.5′	-71°09.0′

Table 2.2. SeaSoar data used for SSP calculations.

III. NUMERICAL MODELING FOR STUDY

This chapter presents an overview of the parabolic equation (PE) model used in the study for propagation modeling. The Monterey-Miami Parabolic Equation (MMPE) model is the acoustic propagation model used throughout this thesis. It is an upgraded version of the University of Miami Parabolic Equation (UMPE) model (Smith and Tappert, 1994) which uses the split-step Fourier (SSF) numerical algorithm. In contrast to separation of variables methods that are based on the approximation that the ocean is horizontally stratified, the parabolic approximation retains full coupling between the waveguide modes, making it valid and highly efficient for more realistic non-stratified oceans and shallow-water applications (Smith and Smith, 1997).

A. GENERAL PE THEORY

In a shallow-water environment where the range is much larger than the depth, the use of cylindrical coordinates is favoured over other coordinate systems. A time-harmonic acoustic field in a cylindrical coordinate system can be represented by

$$P(r,z,\phi,\mathrm{t})=\mathrm{p_f}(r,z,\phi)e^{-i2\pi ft}, \tag{3.1}$$

where p_f (r,z,ϕ) is the frequency dependent pressure amplitude as a function of radial range r, depth z, and azimuthal bearing ϕ. Substituting Eq. (3.1) into the wave equation with a point source leads to the Helmholtz equation

$$\frac{1}{r}\frac{\partial}{\partial r}r\frac{\partial p}{\partial r}+\frac{1}{r}\frac{\partial^2 p}{\partial \phi^2}+\frac{\partial^2 p}{\partial z^2}+k_0{}^2n^2(r,z,\phi)p=-4\pi P_0\delta(\bar{r}-\bar{r}_s) \tag{3.2}$$

where $k_0=\frac{\omega}{c_0}$ is the reference wavenumber $n(r,z,\phi)=\frac{c_0}{c(r,z,\phi)}$ is the acoustic index of refraction, c_o is a reference sound speed, and $c(r,z,\phi)$ is the acoustic sound speed. The source function is represented as a point source at coordinates ($r=0$, $z=z_s$) with reference source level P_o defined as the pressure amplitude at a reference distance of R_o=1m.

If one can assume that the ocean acts as a waveguide then the acoustic energy propagates outward from acoustic sources in the ocean primarily in the horizontal direction. Therefore the pressure field can be approximated by

$$P_f(r,z,\phi)=\Psi_f(r,z,\phi)H_0^{(1)}(k_0r), \tag{3.3}$$

where Ψ_f (r,z,ϕ) is a slowly varying function that modulates the outgoing Hankel function of the first kind. In the far-field, one can take advantage of the asymptotic approximation of the Hankel function and rewrite Eq. (3.3) as

$$P_f(r,z,\phi)=P_0\sqrt{\frac{R_0}{r}}\Psi(r,z,\phi)e^{ik_0r}. \tag{3.4}$$

This is the standard definition of the so-called "PE field function" normalized such that at $r=R_o$, $|\Psi|=1$ and $|p|=P_o$.

Substituting Eq. (3.5) into the Helmholtz Equation (3.2) yields

$$\frac{\partial^2\Psi}{\partial r^2}+i2k_0\frac{\partial\Psi}{\partial r}\frac{1}{r^2}\frac{\partial^2\Psi}{\partial\phi^2}+\frac{\partial^2\Psi}{\partial z^2}\left[k_0^2(n^2-1)+\frac{1}{4r^2}\right]\Psi=0, \tag{3.5}$$

where the source function on the right hand side has been dropped for simplicity. The influence of the source term is only significant at range r=0 and can be accounted for with proper definition of the starting field. Neglecting the azimuthal

coupling and the far-field terms, and assuming that Ψ is slowly varying with range, leads to

$$\frac{\partial \Psi}{\partial r} = \frac{i}{2k_0}\frac{\partial^2 \Psi}{\partial z^2} + \frac{ik_0}{2}\left(n^2 - 1\right)\Psi. \tag{3.6}$$

Defining the operators

$$T_{op} = -\frac{1}{2k_0^{\,2}}\left(\frac{\partial^2}{\partial z^2}\right), \tag{3.7}$$

and

$$U_{op} = -\frac{1}{2}\left(n^2 - 1\right), \tag{3.8}$$

Eq. (3.6) can be written as

$$\frac{i}{k_0}\frac{\partial}{\partial r}\Psi_f(r,z,\phi) = \left(T_{0p} + U_{0p}\right)\Psi_f(r,z,\phi). \tag{3.9}$$

Using the operators defined above, this constitutes what is commonly referred to as the "standard" parabolic equation (SPE) (Tappert, 1977). For this work, the higher order "wide angle" parabolic equation (WAPE) (Thompson and Chapman, 1983) is employed with operators defined by

$$T_{WAPE} = \frac{-1}{k_0^{\,2}}\frac{\partial^2}{\partial z^2}\left[\left(1 + \frac{1}{k_0^{\,2}}\frac{\partial^2}{\partial z^2}\right)^{1/2} + 1\right]^{-1} \tag{3.10}$$

and

$$U_{WAPE} = -\left(n - 1\right). \tag{3.11}$$

The WAPE is the most commonly used PE model today and, although considered accurate to ±40º, it still has its limitations (Smith and Tappert, 1994). The WAPE features less sensitivity to the choice of reference sound speed which

has been an ambiguous feature of most PE models. This is one of the reasons why the WAPE is used in the MMPE model.

B. MONTEREY-MIAMI PARABOLIC EQUATION MODEL

Like the UMPE, the MMPE uses a split-step Fourier (SSF) algorithm to numerically integrate the solution in range. This involves alternatively applying the U_{op} and the T_{op} operators in the z-domain and the k_z-domain, respectively, where each operator is simply a scalar multiplier. The algorithm for stepping in range from r to r+Δr can then be succinctly expressed as

$$\Psi_f(r+\Delta r,z)=e^{ik_0\Delta r\,U_{WABE}(r,z)}\;FFT\left(e^{ik_0\Delta r\hat{T}_{WAPE}(r,k_z)}\left[FFT^{-1}(\Psi_f(r,z))\right]\right), \tag{3.12}$$

where FFT and FFT^{-1} represent forward and inverse Fourier transforms, respectively, and where the wide angle operator T_{WAPE} in k_z-space is defined as

$$\hat{T}_{WAPE}(k_z)=1-\sqrt{\left(1-\frac{k_z^{\,2}}{k_0^{\,2}}\right)}. \tag{3.13}$$

In order to obtain time-harmonic solutions, multiple single frequency components are computed and combined using Fourier synthesis. For each time harmonic solution, the model output is in the form of complex PE field functions for each frequency and spatial grid point, $\Psi(r_i,z_j)$. This can be converted into complex acoustic pressure values by invoking Eq. (3.4).

The current MMPE model allows flexibility in user environmental parameter inputs. The model divides the environment into three layers: the water column, the sediment layer and the deep bottom layer. For this thesis, the 2-D

model broadband version was used and the deep bottom layer was not considered. In the water column the user can specify the range-dependent sound speed profile. The sediment layer requires definition of the water/sediment bathymetry and range-dependent acoustical parameters sound speed, sound speed gradient, density, compressional attenuation, shear speed, and shear attenuation as inputs.

Two types of sources are allowed within the MMPE – a wide-angle source (approximating a point source) and a vertical line array source that allows steering. Again, source parameters need to be specified such as depth, center frequency, bandwidth, and the number of discrete frequencies which generally must be a power of two for efficient FFT computation. If an array length of zero is specified, the model defaults to the wide-angle source. The main input file specifies the names of the other files used in the model and must exist. This includes names of environmental files, output binary files, and computational parameters such as grid-size, range and depth and reference sound speed. The output consists of one single binary file that provides necessary header information on the calculation for post-processing. The majority of the file is the PE field function, Ψ, that is evaluated on the output grid at the discrete set of frequencies requested.

Post-processing of the output data is accomplished using Matlab routines which can extract complex acoustic pressure values anywhere within the environment. For a more detailed description of the model, the reader can download the current existing supporting documentation from the Ocean

Acoustic Library web page http://oalib.njit.edu/pe.html which is supported by the U.S. Office of Naval Research.

IV. PRELIMINARY DATA ANALYSIS AND PROCESSING

In order to determine the broadband nature of the propagation and example TL received at the NW VLA from the raw SUS data, some initial processing and analysis had to be performed. In this thesis, two main data sets, provided by WHOI, were used in an attempt to accomplish the main goal – one that contained SeaSoar data called *Primer3.mat* and another data set that contained the SUS signals for the entire summer cruise. Only a small portion of the data pertaining to the SUS of interest was used. Ambient noise in the area also had to be determined in order to assess whether relative TL comparisons could be achieved. To determine TL received at the VLA, a theoretical curve for energy density level had to be determined, and SSP's and bathymetry profiles had to be generated for MMPE model input.

A. PRIMER ENVIRONMENTAL DATA PROCESSING

The Matlab file p*rimer3.mat* contains the preliminary SeaSoar data collected from the summer cruise. A *read file* provided by WHOI indicated that this data was generated by averaging over 6 minutes in time and 2 m in the vertical. Once the Matlab file is loaded, the following variables of interest are available: sal (salinity), theta (potential temperature), txy (time and position) and pres (ambient pressure). Other data was available but not used in this thesis. An attempt was made to temporally and spatially match the corresponding environmental data to the SUS positions. Unfortunately, in some cases, data was not available (i.e., Run 1 SUS drops) or there was a time lag up to 12 hours

and position offset, as in the case of Run 4 SUS drops. Nevertheless, the usable data was entered as input to a bathymetry extraction program to determine bathymetry profiles and SSP's were produced in proximity to each SUS of interest.

To calculate the SSP's the following commonly used empirical formula was applied (Clay and Medwin, 1977):

$$c = 1449.2 + 4.6T - 0.055T + 0.00029T + (1.34-0.01T)(S-35) + 0.016Z \qquad (4.1)$$

where c= sound speed (m/s), T= temperature(°C), S= salinity (parts per thousand ‰), and Z= depth (m). Examples of typical bathymetry profiles and SSP's used are included as Figures 4.1 through 4.3. These profiles were used as input to the MMPE model.

Note that although there was a better temporal and spatial match with Run 1 SUS data (upslope), there were gaps in the data set due to fishing net avoidance or equipment malfunctions. Therefore, only selected SSP's were produced. This limited the model comparison somewhat. Conversely, for Run 4 along the 90 m isobath, there was increased availability of data but it lacked the spatial and temporal match. Thus, an average of 2 adjacent SSP's were used to input into the model.

Also, no sound speed data were available exactly at the receiver position. In order to define a typical SSP near the VLA, one was chosen as close to the VLA as possible that contained usable data down to the ocean bottom. This profile was also used as input for the 2 SSP model runs discussed later.

As can be seen from the SSP's displayed in Fig. 4.1, there was a sound channel axis present in the region that spanned from about 10-20 m down to the bottom depth. The top receiver of the array (30.5 m) was therefore in the channel while the SUS source detonation (18.3 m) was above the channel in all cases. Thus, all acoustic energy was bottom interacting. This may be a factor when comparing with model results, especially when some uncertainty might exist in the SSP and bottom parameters.

B. ACOUSTIC ENERGY FLUX AND ENERGY SPECTRUM

From the raw data provided, the Matlab file records that matched the SUS of interest were extracted. Each record contains one variable (data) containing a 16 x 32768 double array of SUS complex pressure signals, referring to the number of elements in the array and the number of samples, respectively. As previously discussed, only the top 8 elements contained usable data. This data was used to calculate average energy spectra plots and average energy flux densities.

Urick (1975), based on Weston's work (1960), discusses the necessity to describe an explosion as a source of sound in terms of its acoustic energy flux density in order to avoid the complication caused by propagation effects. The energy density of a plane wave is

$$E = \frac{1}{\rho c}\int_0^\infty p^2(t)dt, \tag{4.2}$$

where p(t) = pressure time series, ρ = density of the medium, and c = sound speed of the medium. The total acoustic energy in the shock wave can be found

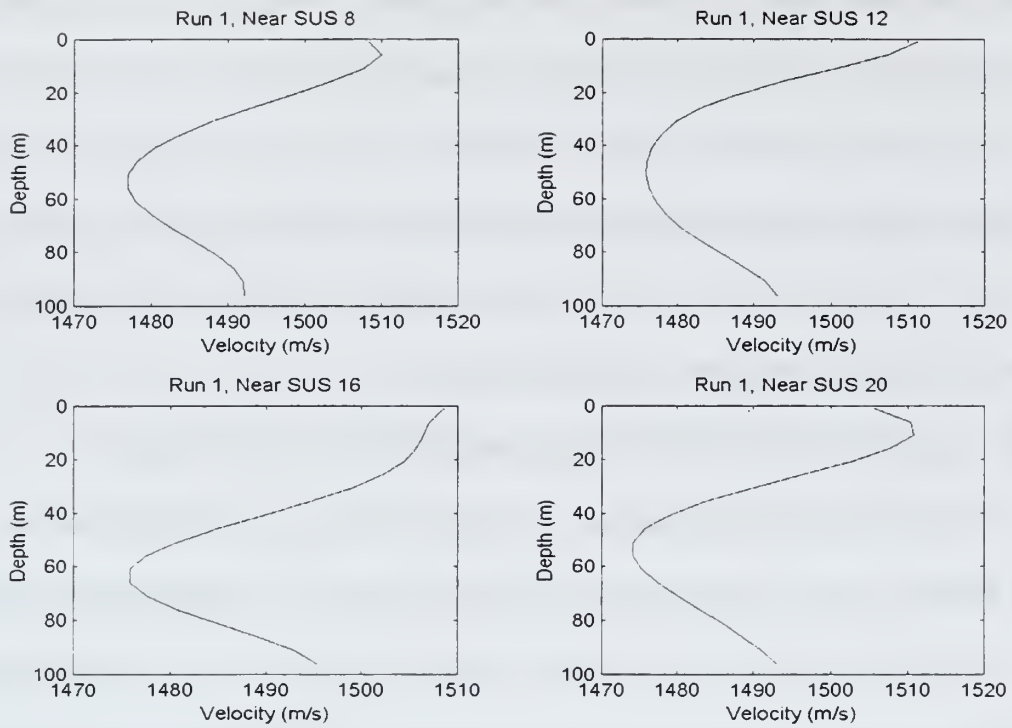

Figure 4.1. Typical SSP's for Run 1 for selected SUS on a N-S track.

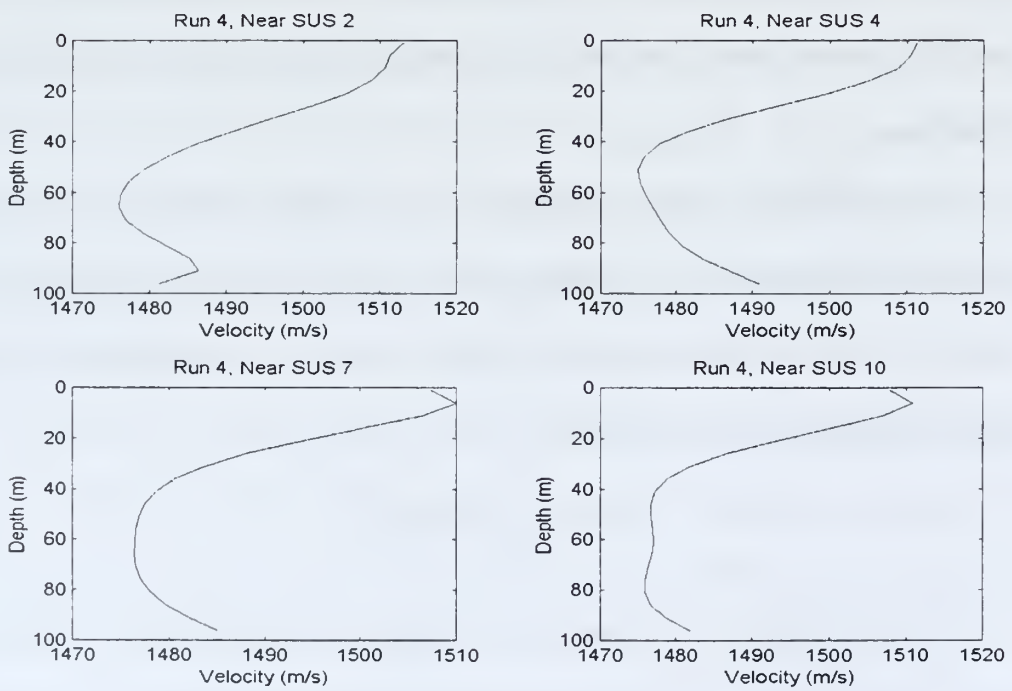

Figure 4.2. Typical SSP's for Run 4 for selected SUS on a W-E track.

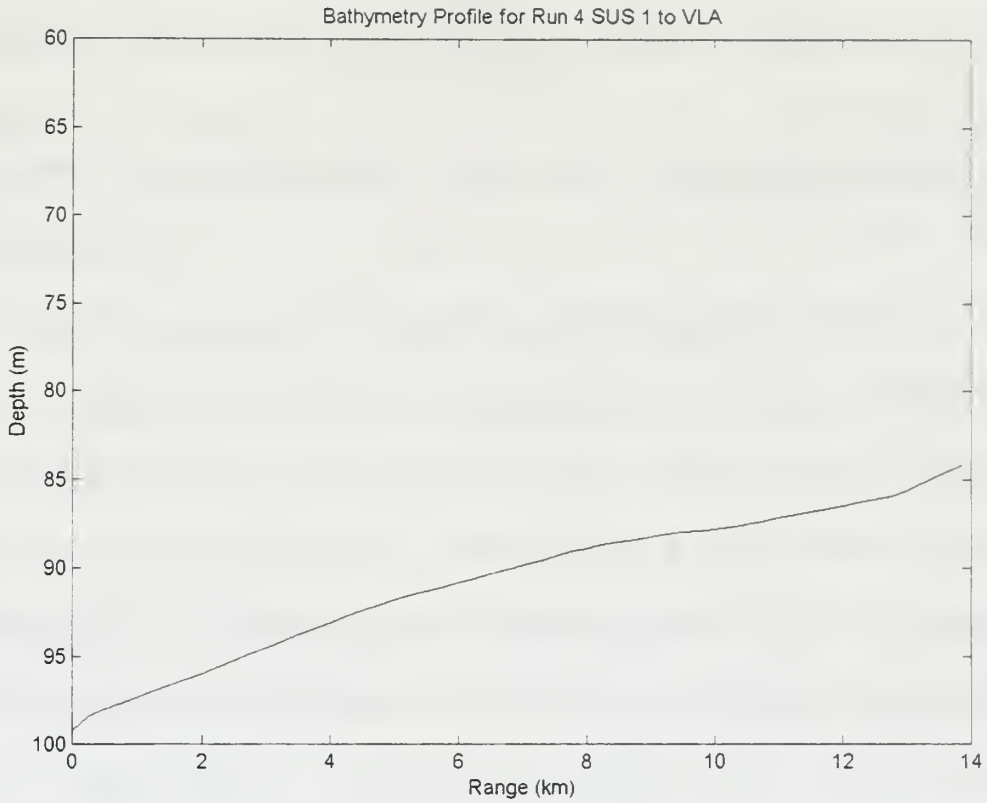

Figure 4.3. Typical Bathymetry profile generated for input into MMPE model.

by substituting the expression $p(t)=P_0e^{-t/t_0}$ in the integral expression (Eq. 4.2) for E. The result is

$$E=\frac{P_0t_0}{2\rho c} \tag{4.3}$$

Since broadband reception is employed with explosive sources, it is convenient to consider the frequency distribution of the acoustic flux energy density of an explosive source. Weston (1960) showed that for an exponential pulse of peak pressure p_o and time constant t_o, the energy flux spectral density $E_0(f)$ can be found using Fourier analysis to be

$$E_0(f) = \frac{2P_0^2}{\rho c\left(\frac{1}{t^2} + 4\pi^2 f^2\right)}. \qquad (4.4)$$

These values were plotted in Fig. 4.16 in Urick (1975) for a 1 lb. charge SUS in units of dB re (1 dyn/cm^2)^2.(s) at 1 yd. Fig. 4.17 in Urick shows explosive spectra for a number of charge weights in dB re 1μPa^2.s at 1 yd. For this thesis, a theoretical curve was extracted from Urick's curves on page 89 for a 1.8 lb. SUS charge. Values in units of dB re (1μPa)^2.s at 1 yd. were interpolated and the curve smoothed using a polyfit function. The resulting Fig. 4.4 was used to compare to SUS data energy spectral density results, E(f). Transmission loss (TL) can then be defined in terms of these spectral densities according to

$$TL(f) = 10\log\left(\frac{E_0(f)}{E(f)}\right). \qquad (4.5)$$

In order to match units, the SUS data had to be multiplied by a scaling factor of 10^8 to convert the WHOI VLA volts amplitude signal to microPascals (i.e. VLA hydrophone sensitivity is –170 dBV re 1 μPa). Fig. 4.5 shows a typical spectrogram taken over a frequency range of 100 Hz to 1000 Hz sampled at 3906.25 Hz sampling rate over 8.33 sec. Only the mid-depth, fourth array element is shown here at a depth of ~ 50 m. This corresponds with the approximate channel axis where the maximum energy would be trapped. Note that more energy is received at lower frequencies.

To compute the energy flux, the pressure amplitude squared was integrated over the time of duration of the signal. Using a Hanning window taper at the ends (64 bins at beginning and end) to smooth the resulting data, we

perform an FFT of the squared pressure data. This will determine the energy flux for each SUS. The resulting data array was saved for further processing to subtract from the theoretical curve extracted from Urick. The theoretical curve had to be interpolated to match the number of data points with the SUS data for further processing.

Due to the variable mode structure over the bandwidth of interest, a single element in depth may not provide a reasonable estimate of typical TL values for a given source/receiver configuration. Therefore, an average of the energy flux spectra over the aperture of the array is computed and used in this analysis. Fig. 4.6 is a typical plot of the energy flux spectrum (in dB re $1\mu Pa^2/Hz^2$) integrated over the depth of the array elements. Note the higher energy flux over the lower frequency range (<500 Hz). Figs. 4.7 and 4.8 show the energy flux versus frequency for selected SUS for respective Runs. This average energy flux data was then subtracted from the theoretical curve to obtain estimates of average TL values versus frequency.

C. AMBIENT NOISE DETERMINATION

In contrast to well-defined levels of deep water ambient noise (AN), ambient levels in coastal waters are subject to wide variations (Urick, 1986). At a given frequency, ambient noise can be attributed to a mixture of shipping and industrial noise, wind noise and biological noise. This also varies with time and space. Therefore, only a rough indication of AN can be given in the MAB area during the experiment.

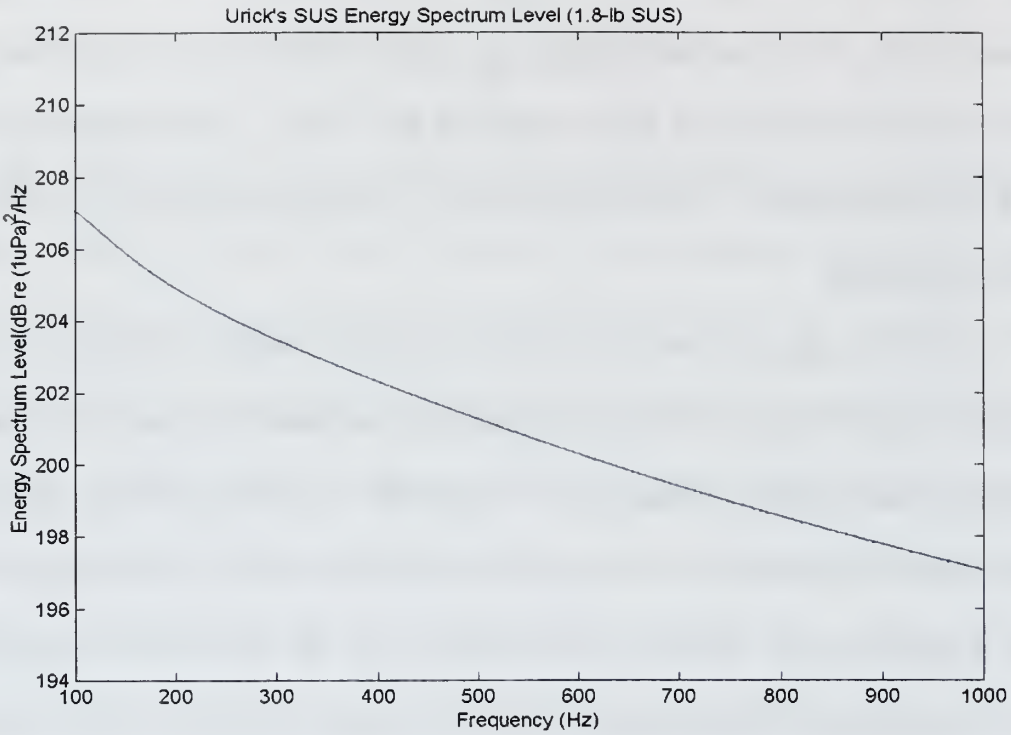

Figure 4.4. Theoretical curve extracted from (Urick, 1975, p. 89) and interpolated manually for 1.8 lb. SUS charge weight.

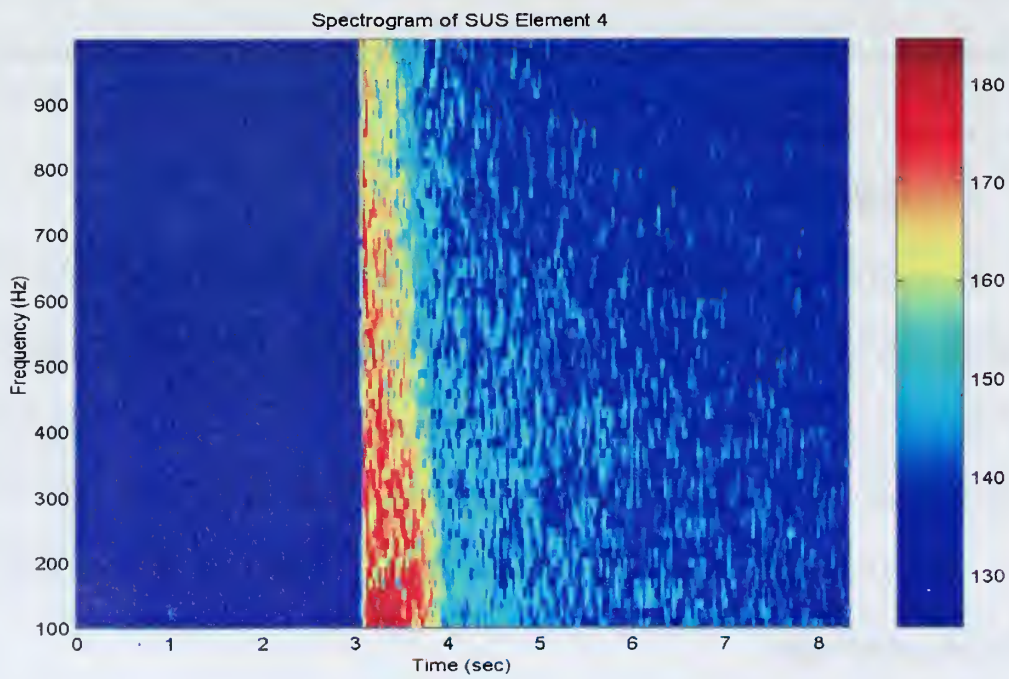

Figure 4.5. Typical spectrogram sampled at 3906.25 Hz sampling rate over 8.33 sec. showing mid array element.

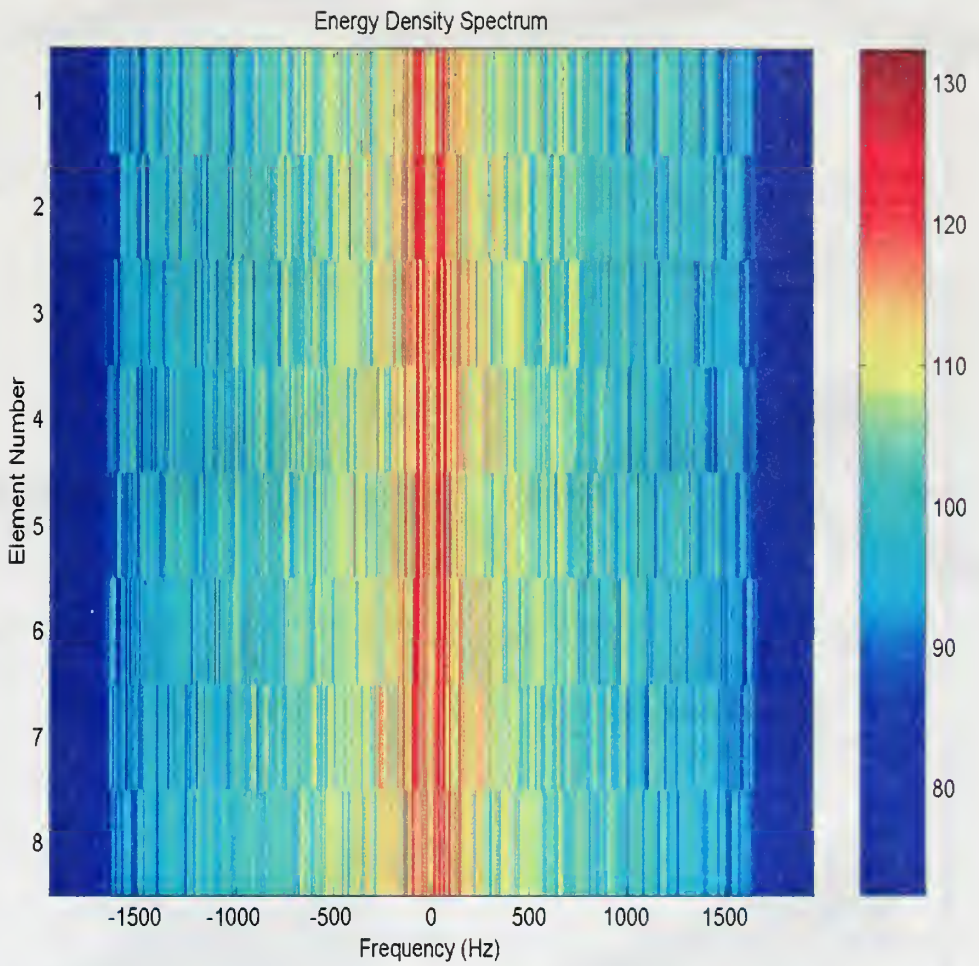

Figure 4.6. Typical energy flux over depth of array elements with higher energy flux at lower frequencies (<500 Hz).

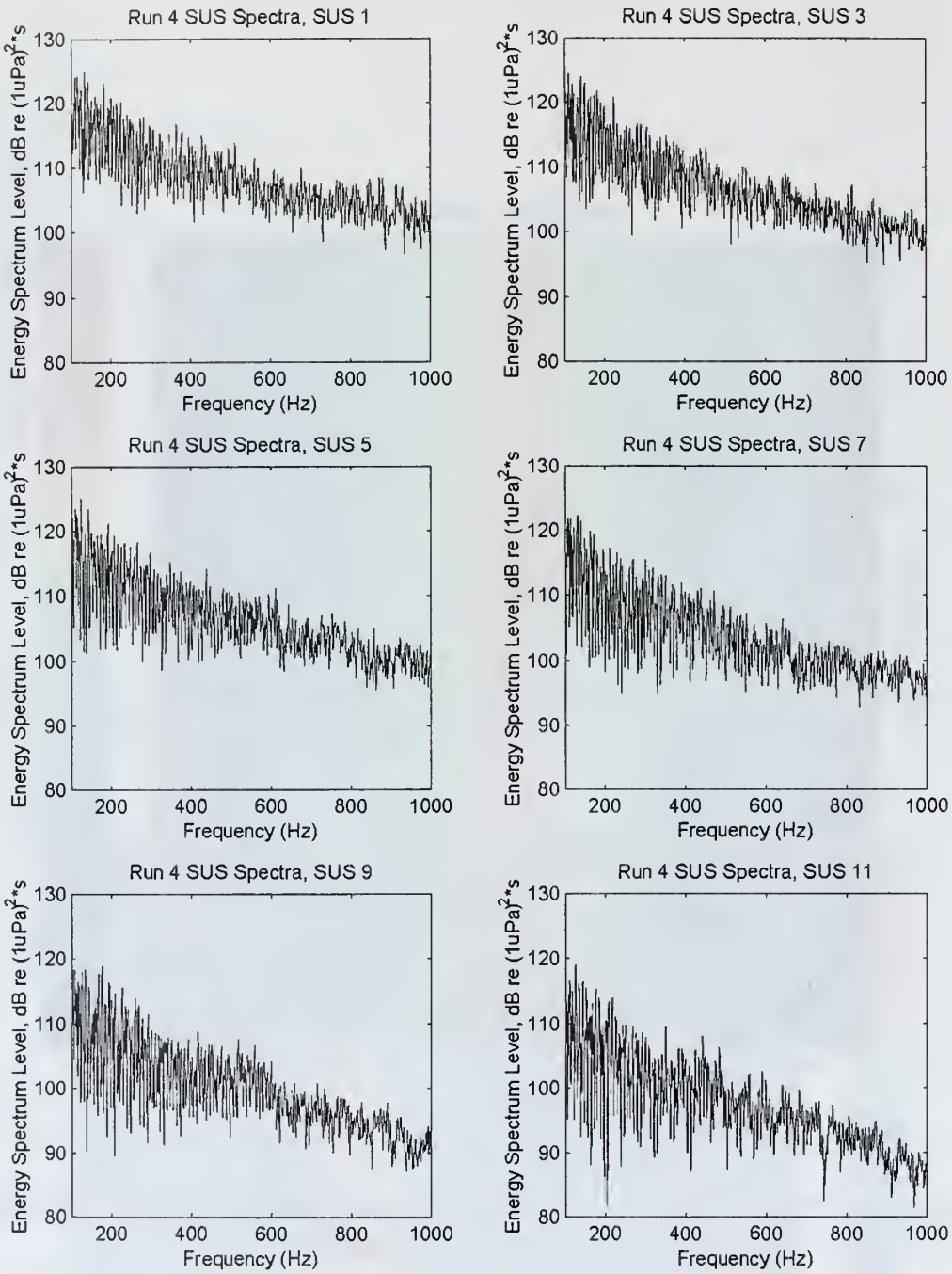

Figure 4.7. Typical SUS energy spectra levels for selected Run 4 SUS data.

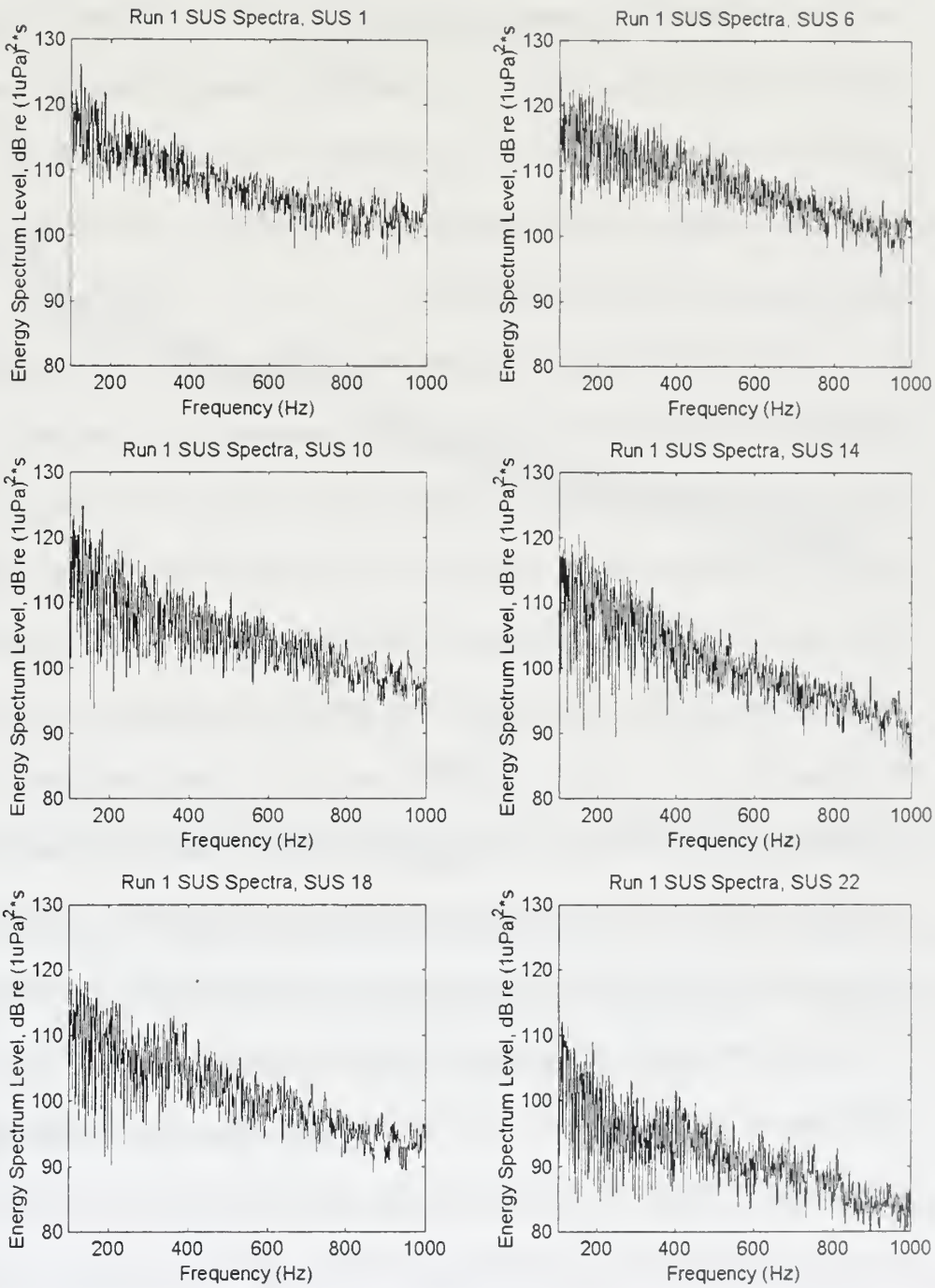

Figure 4.8. Typical SUS energy spectra levels for selected Run 1 SUS data.

One way to measure AN is to use the same SUS data records that were used to calculate the energy spectra for the SUS. Although, once the SUS explosion takes place, there is considerable energy injected into the ocean. However, immediately prior to the explosion, the data record is relatively free from SUS energy. By calculating the spectrum level here, a reasonable determination of AN can be achieved.

Several SUS data records were selected and averaged in depth for all 8 usable VLA elements and then an overall average of the final spectrum level for the 6 selected SUS records. A determination of AN in the area was necessary to ensure that AN was at the expected level and lower than the SUS spectra levels so as to not affect the subsequent TL calculations. Similar to the method used to calculate the SUS spectra, the signal amplitude squared was integrated over time just prior to the SUS explosion, and a FFT was performed to derive the spectrum level for the AN. The averaged result is shown in Figure 4.9. Previous work by Knudsen (1948) and Piggot (1965) in coastal areas off New York and the Scotian Shelf revealed spectrum levels at ~ 90 to 85 dB re 1m over the same 100 to 1000 Hz frequency range and results were plotted as shown in Urick (1975). The spectra calculated here are generally at the same levels showing good agreement. Notice two areas of higher spectrum levels at ~220 Hz and ~ 420 Hz. This elevation is attributed to the transceivers in the water used during the experiment – a 400 Hz (100 Hz bandwidth) moored source and a 224 Hz (16 Hz bandwidth) moored source that were not considered acoustical elements for this thesis. Also, there is a general trend of decreasing AN at higher frequencies, as

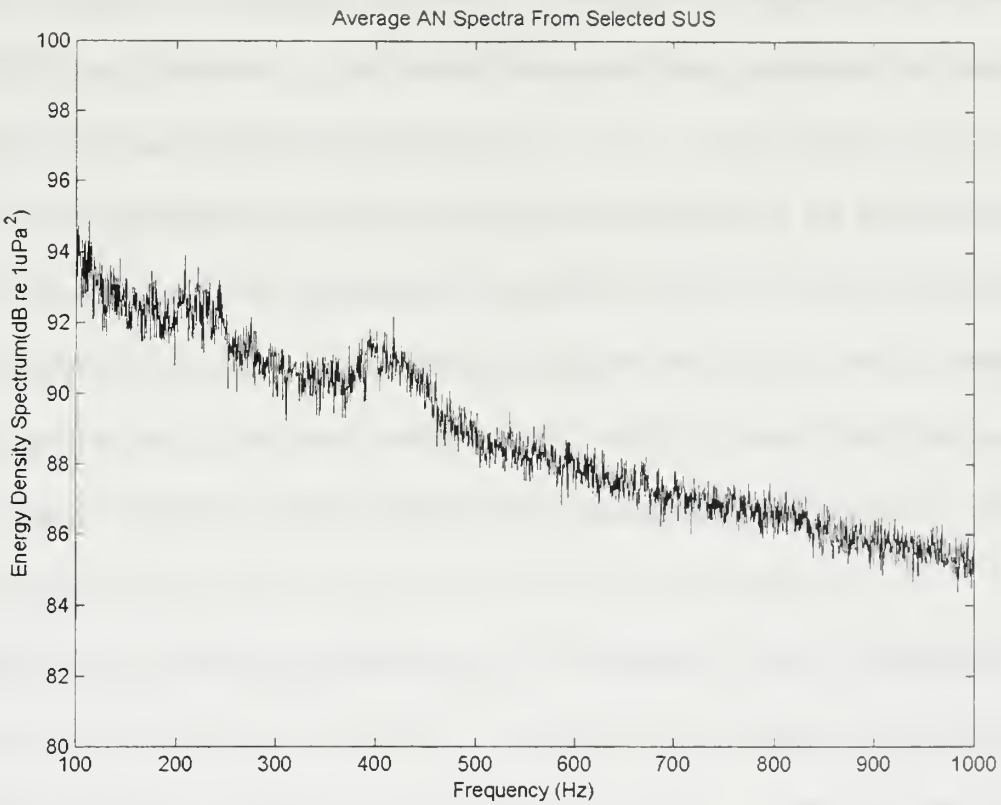

Figure 4.9. Average AN spectra level from selected SUS data used in the study.

one would expect. When comparing the AN spectra with the SUS spectra, the AN spectra is well below the SUS energy spectra by 30-40 dB. Therefore, AN should not be a factor when determining TL for the SUS data.

D. MODEL INPUT AND CASES

Chapter III discussed the theory behind the MMPE and the basic components of the model. Here, the model inputs and case considerations used to compare with the real SUS data results will be discussed. Aside from the SSP and bathymetry input required for the model, the source inputs, the bottom properties, the minimum and maximum depth and range parameters, the

frequency range and center frequency, the number of frequencies, and the source depth had to be included. The model computed CW acoustic propagation over the same frequency range – 100 to 1000 Hz - with a source depth of 18.3 m. The total number of CW runs (number of frequencies) computed by the model was 64, considered a minimum number to provide adequate frequency sampling. (Note the model defaults to a power of 2). The maximum range for each model run was determined by the range of the SUS to the VLA which ranged from ~6 km to ~ 40 km. This resulted in model time runs ranging from 10 min to ~ 2 hrs. The reference sound speed was 1500 m/s for all runs.

To investigate the influence of various environmental factors on the propagation, several combinations of geoacoustic parameters and sound speed profiles were used as modal inputs. A simple bottom model used was defined with sound speed c = 1600 m/s, sound speed gradient = 0 m/s/m, density = 1.2 g/cm^3, compressional attenuation = 0.1 dB/km/Hz, and shear and shear loss were not considered. A realistic bottom model was considered which consisted of a change in sound speed gradient = 10 m/s/m and the density = 1.4 g/cm^3. These changes were considered due to work by Smith, et al. (1998) and Potty, et al. (1998) where a gradient of roughly 10 m/s/m was found in the upper 10 m or so of the sound speed profile in the bottom. A high loss bottom model was also considered which differed from the realistic bottom by doubling the attenuation to 0.2 dB/km/Hz.

Six cases were considered for the model runs in order to determine the best agreement with the SUS data spectra results. These cases included using

1 range-independent SSP (nearest the SUS location) and 2 SSP's (nearest the SUS and nearest the VLA) for a linearly interpolated range-dependent sound speed profile. These two sound speed structures were combined with each of the three bottom models described above.

The predicted energy flux data file was produced by computing the complex pressure at the range of the VLA. This data was then further processed by incoherently averaging the pressure magnitude squared over the depths of the array aperture. The result was then run through a smoothing routine over frequency to determine general trends in average TL versus frequency.

V. MEASURED DATA AND MODEL COMPARISON RESULTS

This chapter will discuss the TL results obtained from the measured data and the model runs using the different geoacoustic parameter bottom profiles and environmental cases described in the previous section.

A. MEASURED DATA RESULTS

Once the relevant measured SUS data was processed and the energy spectrum levels were computed, they were subtracted from the theoretical curve extracted from Urick (1975). Figs. 5.1 and 5.2 show typical TL curves for each SUS Run using selected SUS from short to long range (i.e., ~6 km to ~40 km for Run 1 and ~14 km to ~28 km for Run 4). Note that these TL levels are not normalized to absolute values due to the ambiguity in the source level estimation from Urick.

The general trend, which is our main concern in the thesis, seems to be consistent throughout the analysis with TL being lower at shorter ranges (i.e., SUS 1 for both Runs) which is what one would expect. The same is also true with regard to frequency. Lower frequencies at ~100 Hz tended to have lower TL than higher frequencies at ~1000 Hz, and again, this is to be expected since there is generally higher loss at higher frequencies over range.

If two TL profiles relatively equidistant from the VLA are compared, as shown in Fig. 5.3, some observations can be made. The top plot comparing two SUS that are very close in position (see Fig. 1.1) shows a very similar trend and nearly constant dB difference over the bandwidth. The difference in dB is likely

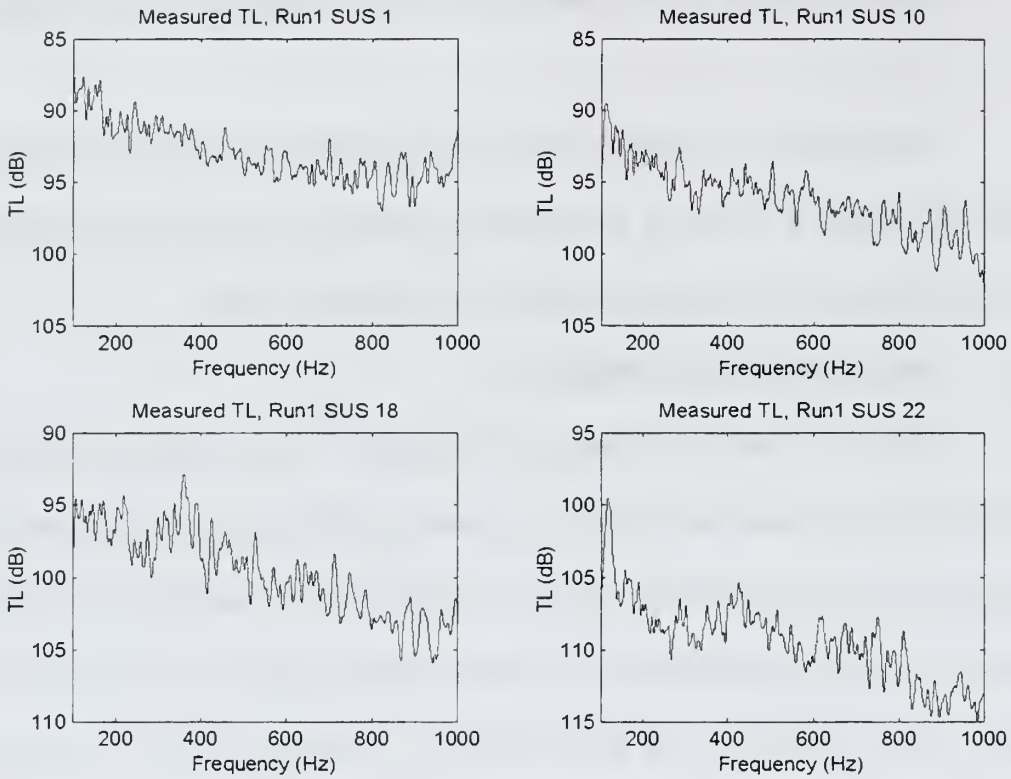

Figure 5.1. TL estimate between Urick's curve and Run 1 selected SUS.

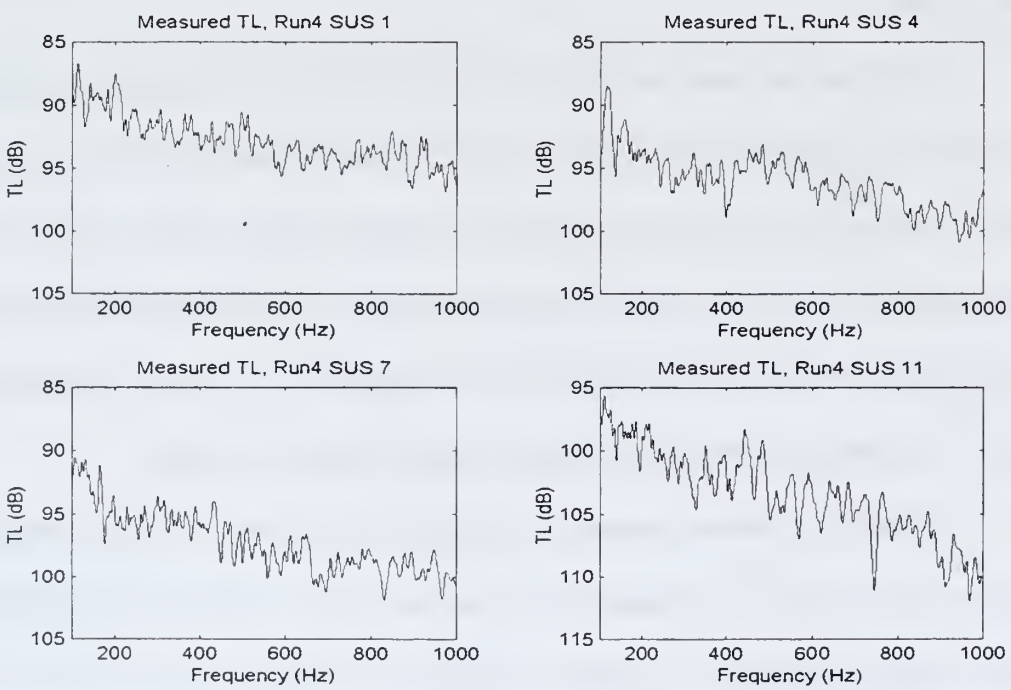

Figure 5.2. TL estimate between Urick's curve and Run 4 selected SUS.

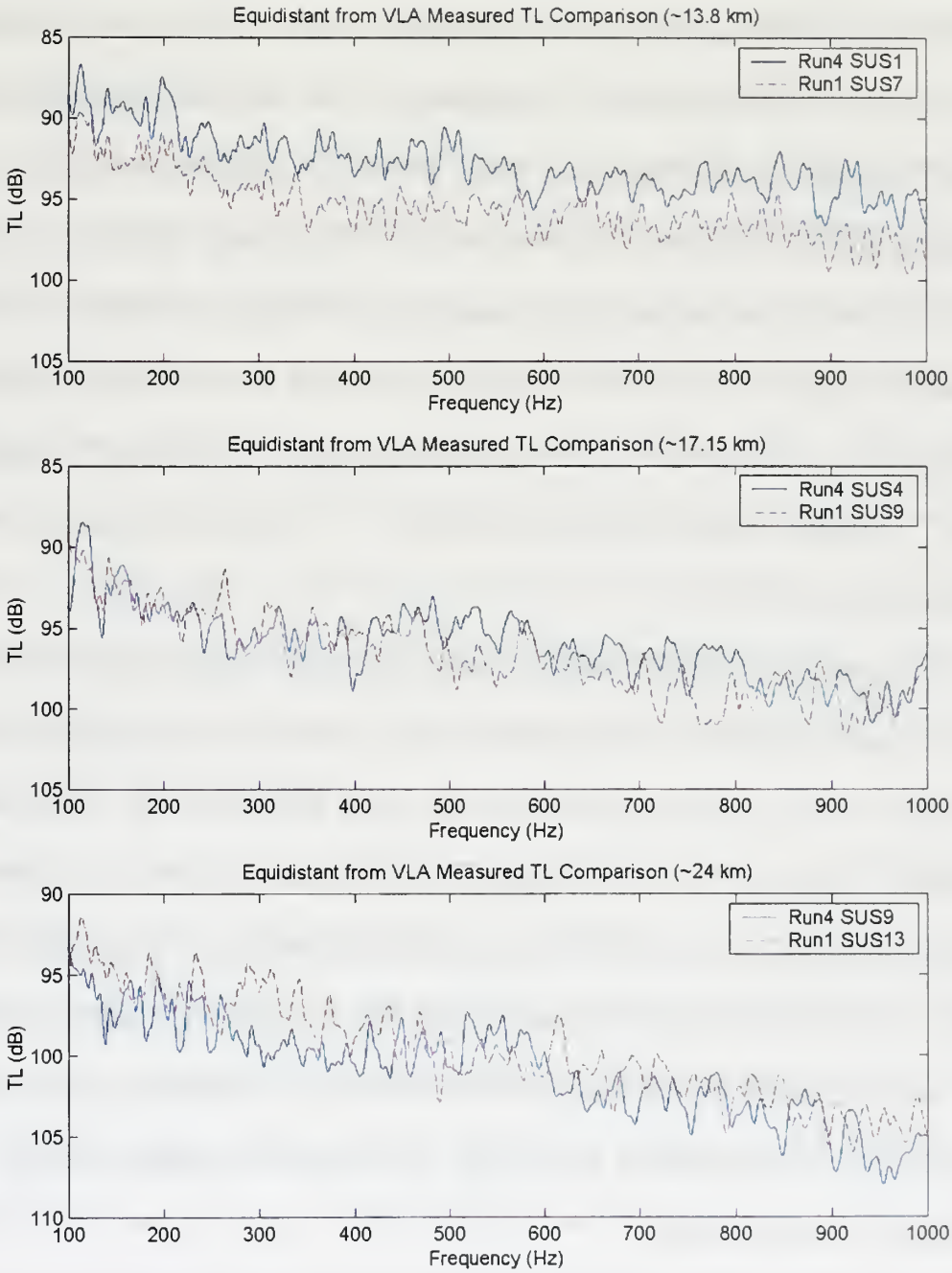

Figure 5.3. Comparison of TL between equidistant SUS from each run.

due to a difference in range between the SUS drop locations. The estimated positions of the SUS drops, as listed in Table 2.1, do not support the level of difference in the first plot of Fig. 5.3. However, errors in the estimated positions may exist which could account for the difference. The other two plots again show similar TL trends over the frequency band, although there is more variation in the oscillation and dB difference between the two. When range offsets (dB offsets) are considered, these last two plots reveal the most significant differences in the frequency range ~500 – 600 Hz. This could be due to the sloping bathymetry along the Run 1 transmissions which becomes more important with increasing range. However, these differences are only ~2 - 3 dB, inferring that the slope had little impact on the TL.

In general, the results from the measured data revealed expected trends in TL for each SUS Run. Range from the VLA receiver was the predominant factor with lower frequencies exhibiting the least amount of TL. One area of uncertainty, however, is in the computed dB levels of the TL. Without a reference source level from the SUS and the ambiguity factor inherent in Urick's curves when extracting the theoretical curve, the resulting TL profiles may have some error in the dB levels. Since the concern was more with the general trend, this was not a requirement but would have been an added bonus when comparing to model results.

B. MODEL VARIABILITY

From the six bottom types used to investigate the influence of environmental factors on propagation, the high loss bottom model using 0.2

dB/km/Hz had the least effect on the predicted TL trend. The results primarily mirrored the lower attenuation results and the TL was increased by ~2 – 10 dB (depending on range) for the 1 SSP and 2 SSP cases. Thus the attenuation results were not included in the following model variability plots.

Figures 5.4 through 5.7 show the model variability results for selected SUS for each Run for the remaining four cases – the simple bottom case and realistic bottom case (indicated by MOD on the figures) for each of the range-independent SSP and for the 2 SSP linearly interpolated range-dependent case. The resulting model TL curves revealed several observations. First, the TL levels were generally 10 – 15 dB different than the measured data due to the ambiguity in the absolute levels of the measured data. Second, the TL curves generally displayed a flatter response than the measured data. These two factors made the comparison to the measured data more difficult as will be shown later in the discussion.

With regard to the variability of the different cases, the predicted TL spread for each SUS was generally low in most cases (i.e., +/- 2 dB). However, there was much more variation with regard to oscillation in the trend as a function of frequency. Also, there was little difference between the simple bottom 1 SSP case and the realistic bottom (MOD), 1 SSP case. Likewise, the 2 SSP cases for both bottom types were very similar in response while the most significant factor on the absolute TL levels was the bottom attenuation. Unfortunately, since the SSP used closest to the VLA was not exactly at the VLA position, and some

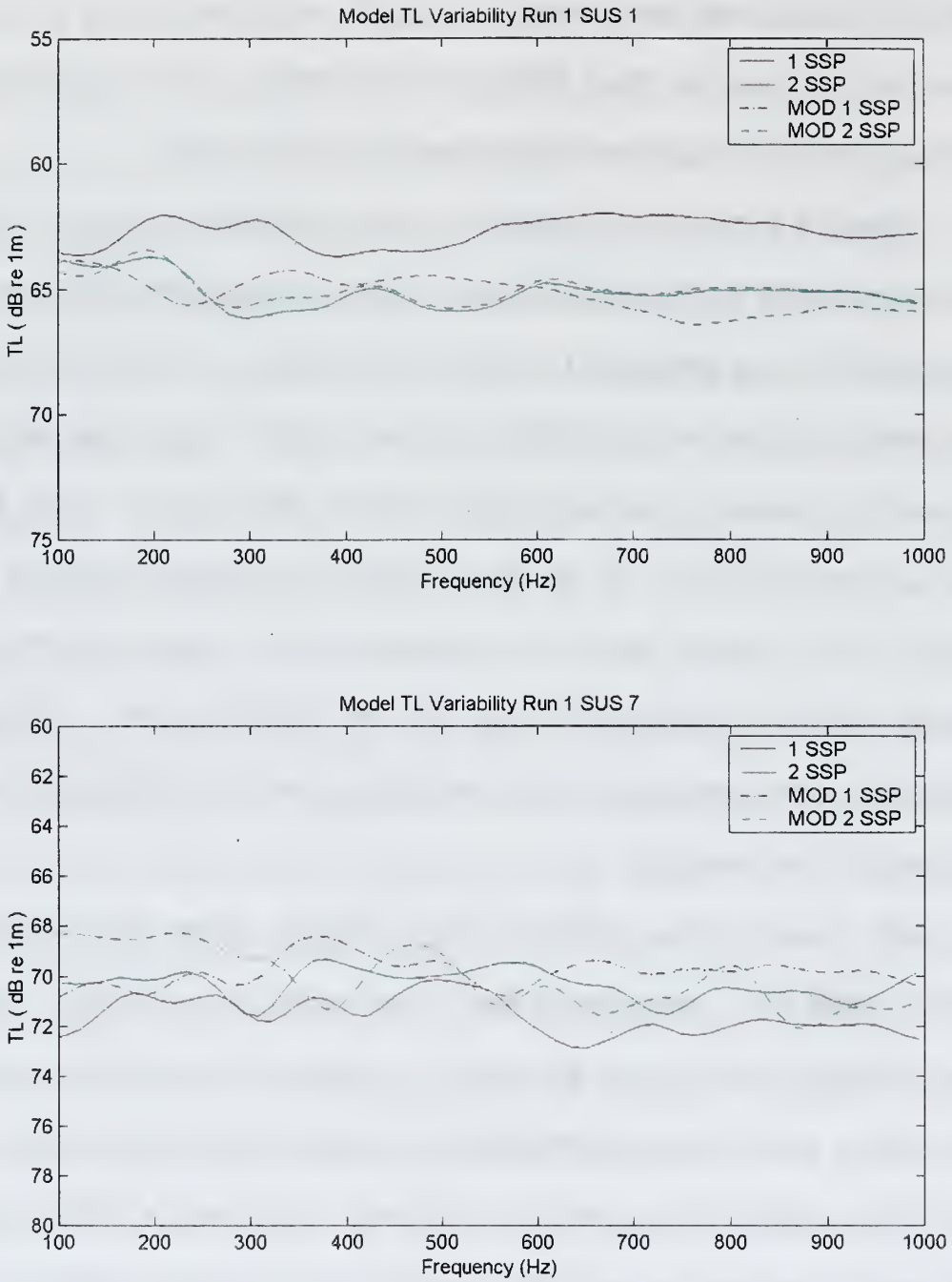

Figure 5.4. Run 1 selected SUS model TL variability (short range).

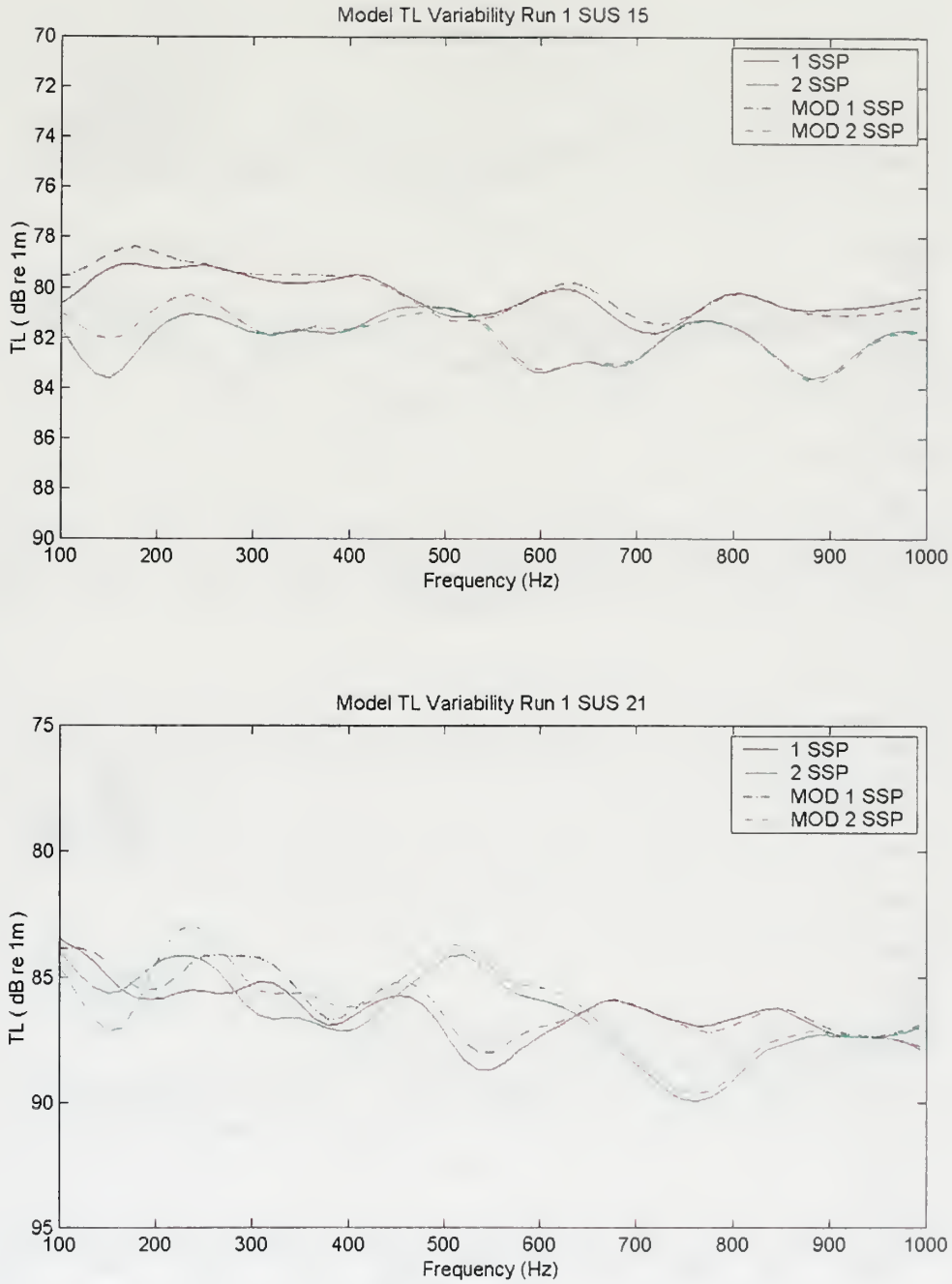

Figure 5.5. Run 1 selected SUU model TL variability (long range).

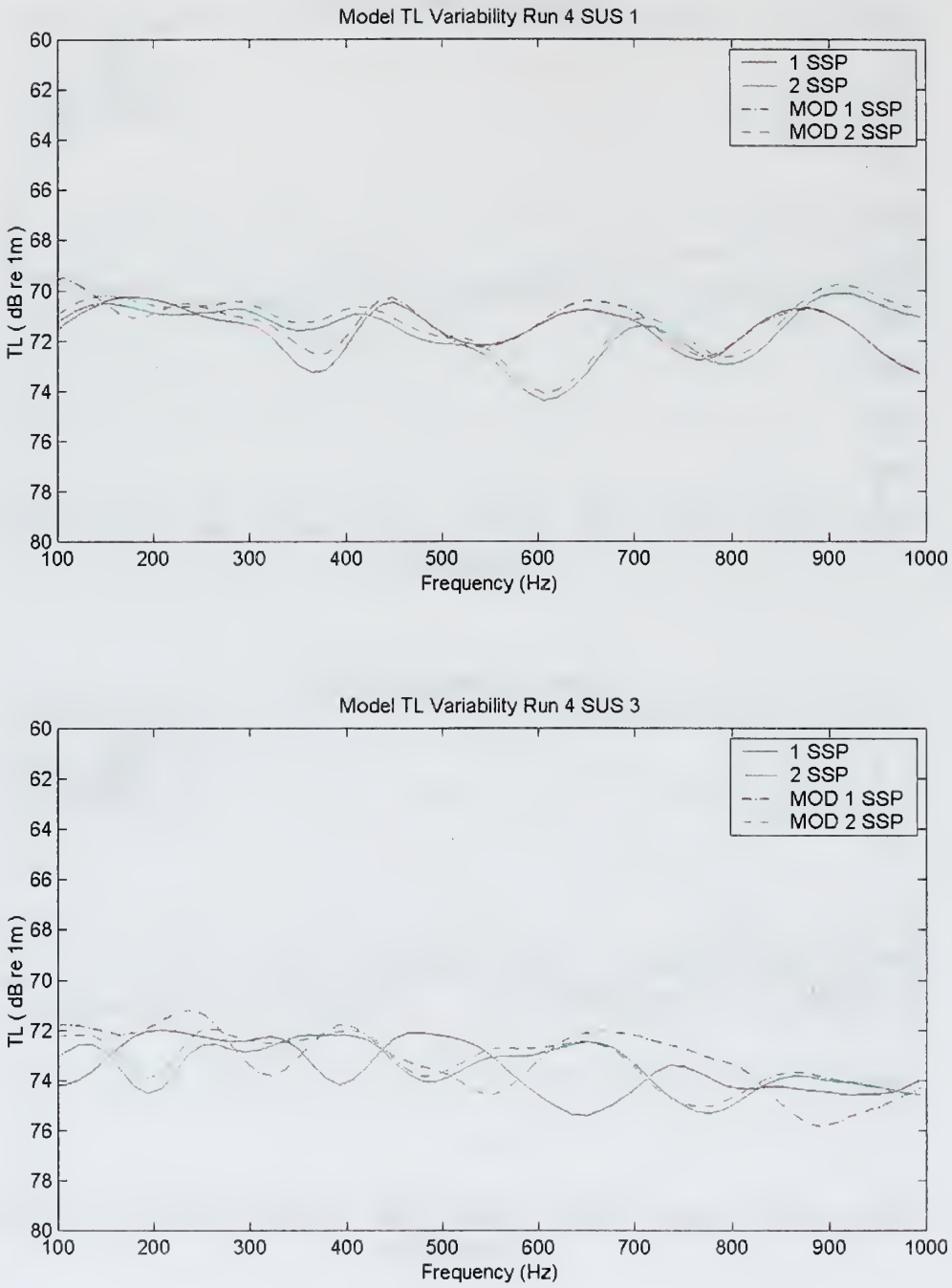

Figure 5.6. Run 4 selected SUS model TL variability (short range).

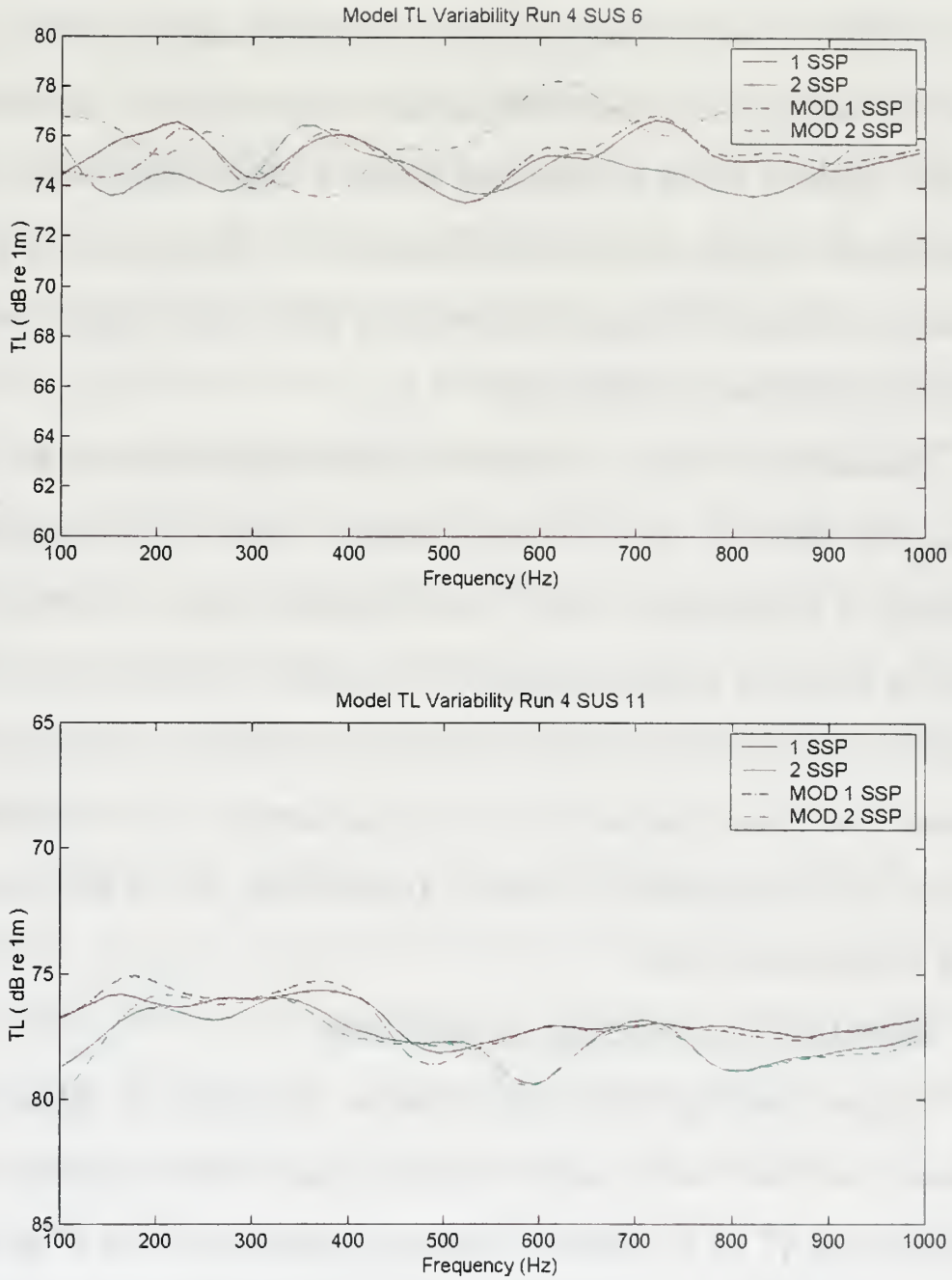

Figure 5.7. Run 4 selected SUS model TL variability (long range).

averaging or interpolation had to be performed on other SSP's used in the model runs, it is difficult to assess the amount of inaccuracy induced in the environment. However, it was noted from the SSP's used as model input that the variation from the SSP closest to the VLA to the ones further in range differed with a slight deepening and widening of the sound channel axis. Although the change was minimal, it may have been significant enough to affect model results in the way the model interpolates the SSP's used.

Generally, there was no significant frequency dependence in any of the cases as the response was most often nearly flat. There was some increasing undulating of TL response, however, with increasing range for both runs. It should be noted that a brief examination of a single run was performed with a change in the bottom sound speed, reduced from 1600 m/s to 1500 m/s. This produced a significant change in the TL trend, generating a ~20 – 30 dB variation in the TL over the bandwidth of interest. Unfortunately, lack of time prevented further analysis of this effect.

C. MEASURED DATA/MODEL COMPARISON

As was mentioned earlier, the difference in absolute TL values of the measured data and model results, and the greater increasing slope of the measured data TL as a function of frequency compared to that of the model results, made it difficult to match the results. Nevertheless, an attempt was made to show examples of the best and worst matches for each SUS Run. Figs. 5.8 and 5.9 show examples of Run 4 and Run 1 SUS results where the top two profiles show relatively good general trend agreement and the bottom two

profiles show poor agreement.

The plots were produced by using the measured data results as the baseline with the model results superimposed and adjusted in scale to achieve the best fit. The TL levels are not significant here as it was noted that there was generally a 10 – 15 dB discrepancy between the two. By best fit we mean to match the majority of the general trend as best as possible since in most, if not all cases, matching one end of the spectrum was at the expense of the other end. This was especially true with Run 4 results. The best results in Run 4 (Fig. 5.8) were at mid frequency range and did not match up well at either end. On the other hand, Run 1 (Fig. 5.9) showed relatively good agreement with SUS at longest ranges and downslope from the VLA (i.e., SUS 18 and 20). The SUS results at shorter ranges were not as promising as indicated in the bottom two examples.

In most of the results, the 2 SSP environments revealed the poorest agreement. Generally, a much flatter response was observed throughout most of the frequency range. In those cases where the trends seemed to match best, only a single SSP was used. Longer ranges between SUS and VLA positions also seemed to improve the comparisons. The justification for these observations is unclear. However, one may speculate that the primary difference in sound speed profiles occurred over a relatively short range nearer the VLA. Thus the use of a single SSP near the SUS source position would provide more accurate predictions than a linear interpolation between SSP's. Reasons for the poor matches for the short range transmissions are still unclear.

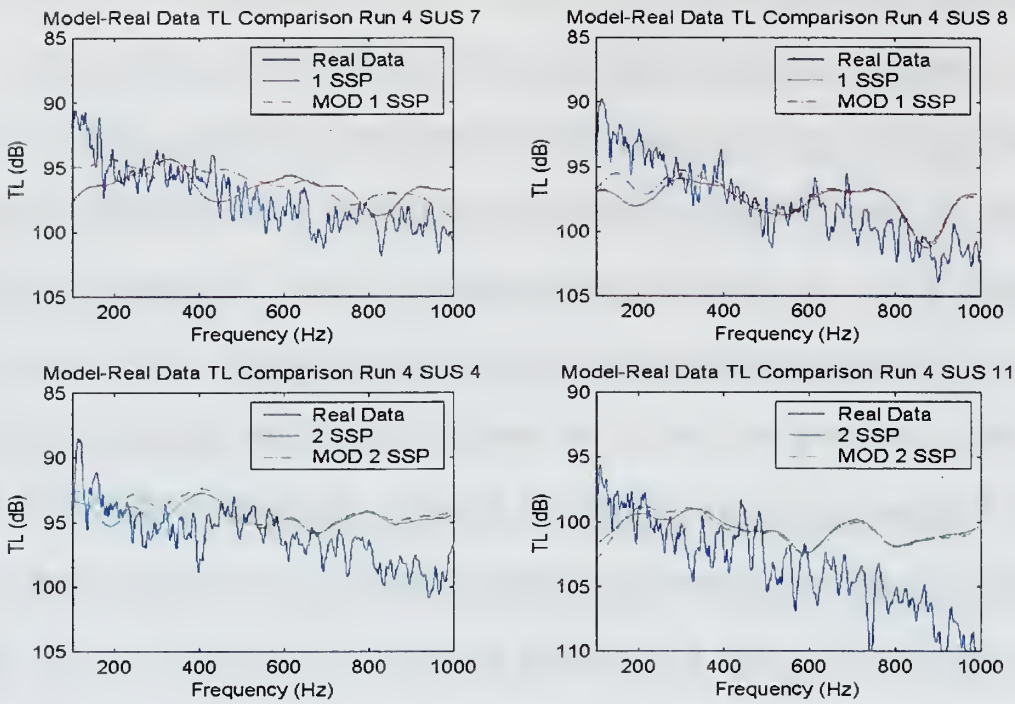

Figure 5.8. Run 4 – Model-measured data TL comparison.

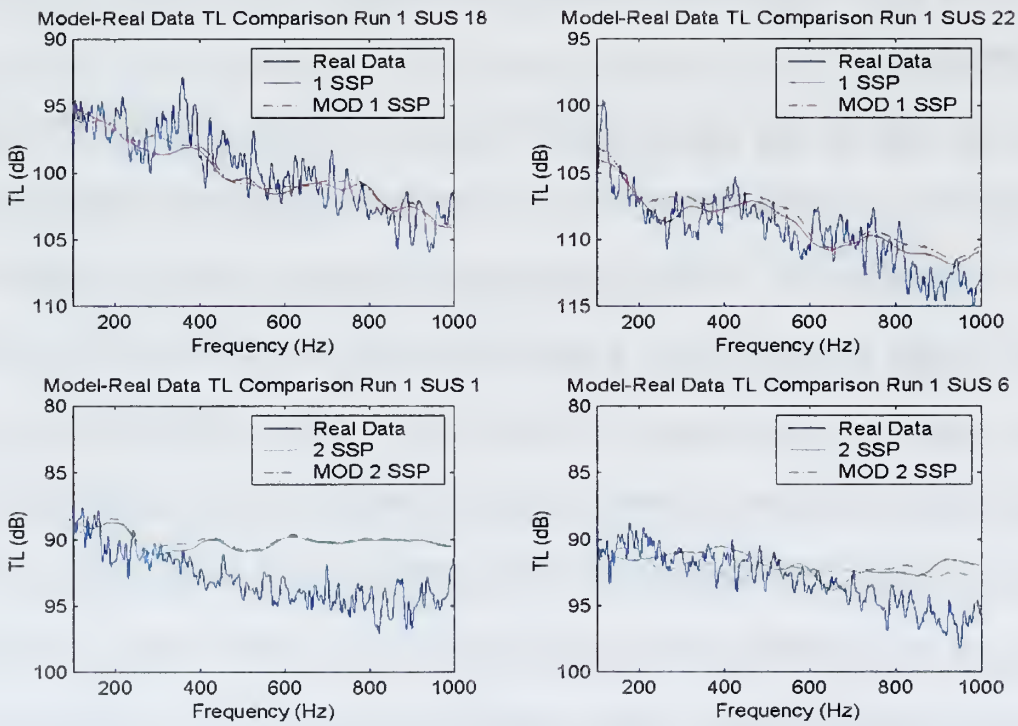

Figure 5.9. Run 1 – Model-measured data TL comparison.

VI. CONCLUSIONS

The 1996 Mid-Atlantic Bight (MAB) Primer experiment was conducted to gain a better insight into shallow water sound propagation by quantifying shelf break frontal variability and its connection with local oceanographic environmental conditions. Part of the experiment required that Signal Underwater Sound (SUS) charges be dropped via aircraft flyover and the broadband signals be recorded for subsequent analysis using a nearby vertical line array (VLA) moored several kilometers to the northwest. This thesis attempted to process and analyze 11 Run 4 SUS signals (along the 90 m isobath) and 22 Run 1 SUS signals (upslope) from data sets provided by Woods Hole Oceanographic Institution (WHOI) and University of Rhode Island (URI) to determine SUS spectra and transmission (TL) estimates using Urick's theoretical curves for a 1.8-lb SUS charge weight. These TL estimates were then compared to Monterey-Miami Parabolic Equation (MMPE) model results for various geoacoustic parameters and range-dependent and range-independent sound speed profile (SSP) cases. The following observations and recommendations can be drawn from the study and analysis:

- Matching exact SSP's with SUS positions for model input proved to be difficult with available data either being incomplete or lacking the spatial and temporal agreement with the SUS drops. The resulting averaging and interpolation of SSP's may have induced some imprecision in model TL results.

- Sound speed profiles revealed a channel axis at ~50 – 60 m in the experimental region where maximum energy is likely to be trapped. The VLA hydrophones were positioned from 31.5 m down to 59 m

within the axis while the SUS was set to detonate at 18.3 m. This most likely reduced the maximum volt signal received at the VLA.

- The lack of a known reference source level for the SUS signals coupled with some unknown ambiguity factor inherent in Urick's theoretical curve made SUS energy flux and subsequent TL estimate difficult to calculate. This unknown error caused a discrepancy in TL values between the measured and model results that made the measured versus model comparison difficult.

- Ambient noise (AN) in the region was determined to be at a typical level for a shallow water environment and well below the SUS spectra energy levels. Therefore, ambient noise was not a factor in preventing accurate TL estimates from measured data. However, since the ambient noise could vary considerably from one shallow water region to the next, it should not be dismissed as a possible factor in the TL measurements.

- SUS energy spectra revealed higher levels at lower frequencies and closer ranges. Thus, TL estimate trends were as expected with longer range transmissions and higher frequencies both showing increased TL.

- MMPE model results were generally ~10 – 15 dB different from measured TL estimates due to lack of absolute SUS source levels. The model results typically showed a much flatter response than measured data.

- Doubling the attenuation factor of the sea bottom had little influence on the model trend results but did influence the absolute predicted TL significantly. The most favourable agreement between measured data TL and model TL resulted when using a single SSP with a simple or realistic bottom profile while results obtained by interpolating between two SSP's showed the poorest agreement.

- The results of this analysis tend to suggest that bottom attenuation dominates absolute levels while the range-dependent sound speed structure dominates the finer scale features in TL over the bandwidth. Although not examined in this thesis, a brief investigation suggested that bottom sound speed at the water/bottom interface may dominate the larger scale trend of TL as a function of frequency.

The goal of follow-on analysis should be to examine more thoroughly the role of the sediment sound speed at the water/bottom interface. In addition, more recent analysis by the Woods Hole group on the oceanographic conditions may provide better range-dependent sound speed structures to improve the resolution of the fine-scale features of transmission loss versus frequency. Finally, an attempt should be made to resolve the missing ambiguity factor in Urick's SUS spectra data. This may allow a matching of absolute TL levels between model and measurement providing an inversion scheme for determining bottom attenuation.

LIST OF REFERENCES

Clay, C. S. and H. Medwin, *Acoustical Oceanography*, John Wiley and Sons, New York, 1977.

Gawarkiewicz, Glen, Robert Pickart, James F. Lynch, Ching_Sang Chiu, Kevin Smith, and James Miller, "The Shelfbreak Front PRIMER Experiment, "*J. Acoust. Soc. Am.,* 101 (5), May 1997.

Hannay, D. E and N. R. Chapman, "Source Levels for Shallow Underwater Sound Charges, "*J. Acoust. Soc. Am.,* 105 (1), Jan 1998.

Jensen, Finn, B., William A. Kuperman, Michael B. Porter, and Henrik Schmidt, *Computational Ocean Acoustics,* New York: American Institute of Physics, 1994.

Kinsler, Lawrence E., Austin R. Frey, Alan B. Coppens, and James V. Sanders, *Fundamentals of Acoustics,* Third Edition, New York: John Wiley & Sons, 1982.

Knudsen, V. O., R. S. Alford, and J. W. Emling, " Underwater Ambient Noise," *J. Mar. Res.*, 7:410, 1948.

Lynch, J. F., G. G. Gawarkiewicz, C. S. Chiu, R. Pickart, J. H. Miller, K. B. Smith, A. Robinson, K. Brink, R. Beardsley, B. Sperry, and G. Potty, "Shelfbreak PRIMER – An Integrated Acoustic and Oceanographic Field Study in the Middle Atlantic Bight, "Proceedings of International Conference on Shallow Water Acoustics, Beijing, China, April 21-25, 1997.

Medwin, Herman and Clarence S. Clay, *Fundamentals of Acoustical Oceanography,* New San Diego, California: Academic Press, 1998.

Pickart, Robert S., Glen G. Gawarkiewiecz, James F. Lynch, Ching-Sang Chiu, Kevin B. Smith, and James H. Miller, "Endeavor 286 Cruise Summary: PRIMER III," 1996.

Piggot, C. L.," Ambient Sea Noise at Low Frequencies in Shallow Water of the Scotian Shelf," *J. Acoust. Soc. Am.*, 36:2152, 1965.

Poag, C. W., " Stratigraphy and Depositional Environment of Baltimore Canyon Trough," *The American Assoc. of Petrolium Geologists Bulletin*, Vol. 63:9, pp. 1452-1466, 1979.

Potty, G. R., J. H. Miller, J. F. Lynch, and K. B. Smith, " Tomographic Mapping of Sediments in Shallow Water," *J. Acoust. Soc. Am.*, 1998.

Robinson, Allan R., Ding Lee, *Oceanography and Acoustics: Prediction and Propagation Models,* New York: AIP Press, 1994.

Smith, Kevin B., James H. Miller, James F. Lynch, Ching-Sang Chiu, "Shelfbreak Primer Quicklook: Acoustic Observations and Modeling Comparison," Naval Postgraduate School, Monterey, CA, 1996.

Smith, Kevin B., José G. Rojas, James H. Miller, and Gopu Potty," Geoacoustic Inversions In Shallow Water Using Direct Methods And Genetic Algorithm Techniques," J. Adv. Marine Sci. and Tech. Soc., 1998.

Smith, Kevin B., Department of Physics, Naval Postgraduate School, Monterey, CA, Personal Communication, 1995.

Urick, Robert J., *Ambient Noise in the Sea,* Los Altos: Peninsula Publishing, 1986.

Urick, Robert J., *Principles of Underwater Sound,* Second Edition, New York: McGraw-Hill, 1975.

Volak, D., B. Brown, E. Zeidler, "Shelfbreak PRIMER 1996," Technical Note TN-SBP-96, 1996.

Wenz, G. M., "Acoustic Ambient Noise in the Ocean: Spectra and Sources, "*The Journal of the Acoustical Society of America, Vol. 34:12, pp. 1936-1956, 1962.*

Ziomek, L. J., *Fundamentals of Acoustic Field Theory and Space-Time Signal Processing,* Boca Raton: CRC Press, 1995.

INITIAL DISTRIBUTION LIST

1. Defense Technical Information Center 2
   8725 John J. Kingman Rd., STE 0944
   Ft. Belvoir, VA 22060-6218

2. Dudley Knox Library 2
   Naval Postgraduate School
   411 Dyer Rd.
   Monterey, CA 93943-5101

3. Chairman, Code PH/Sk 1
   Engineering Acoustics Academic Committee
   Naval Postgraduate School
   Monterey, CA 93943-5101

4. National Defence Headquarters 1
   Mgen George R. Pearkes Building
   Ottawa, Ontario, Canada
   K1A 0K2
   Attention: DPED

5. National Defence Headquarters 1
   Mgen George R. Pearkes Building
   Ottawa, Ontario, Canada
   K1A 0K2
   Attention: DMA3-5

6. Professor Kevin B. Smith, Code PH/Sk 5
   Department of Physics
   Naval Postgraduate School
   Monterey, CA 93943-5101

7. CDR Mitch Shipley 1
   Department of Physics
   Naval Postgraduate School
   Monterey, CA 93943-5101

8. Major Dominic Carino 2
   46 Barron Street
   Welland, Ontario, Canada
   L3C 2K5

60 290NPG TH 2310
6/02 22527-200 NLB

DUDLEY KNOX LIBRARY
3 2768 00403343 1